GENES, CHROMOSOMES & CANCER 46:348–358 (2007)

Mutation and Expression Analyses of the *MET* and *CDKN2A* Genes in Rhabdomyosarcoma with Emphasis on *MET* Overexpression

Yuyan Chen,[1] Junko Takita,[2] Masashi Mizuguchi,[1] Kiyoshi Tanaka,[3] Kohmei Ida,[1] Katsuyoshi Koh,[1] Takashi Igarashi,[1] Ryoji Hanada,[4] Yukichi Tanaka,[5] Myoung-Ja Park,[6] and Yasuhide Hayashi[6]*

[1]Department of Pediatrics, Graduate School of Medicine, University of Tokyo, Tokyo, Japan
[2]Department of Cell Therapy and Transplantation Medicine, Graduate School of Medicine, University of Tokyo, Tokyo, Japan
[3]Department of Surgery, School of Medicine, Kitasato University, Kanagawa, Japan
[4]Division of Hematology/Oncology, Saitama Children's Medical Center, Saitama, Japan
[5]Division of Pathology, Kanagawa Children's Medical Center, Kanagawa, Japan
[6]Division of Hematology/Oncology, Gunma Children's Medical Center, Gunma, Japan

Rhabdomyosarcoma (RMS) is the most common soft-tissue sarcoma of childhood. The simultaneous loss of *Ink4a/Arf* function and disruption of Met signaling in *Ink4a/Arf*$^{-/-}$ mice transgenic for hepatocyte growth factor/scatter factor (*HGF/SF*) induces RMS with extremely high penetrance and short latency. To address the roles of *MET* and *CDKN2A* ($p16^{INK4A}/p14^{ARF}$) in human RMS, we performed mutational analyses in 39 samples of RMS by PCR-SSCP. No mutations were detected in exons 14–21 of *MET* whereas a nonsense mutation at codon 80 of $p16^{INK4A}$ was identified in an alveolar RMS cell line. We also quantified the relative expression levels and DNA copy numbers of these genes in seven cell lines and 17 fresh tumors by real-time quantitative PCR. Expression of *MET* was detected in all samples; however, more than 10-fold difference was found in the samples with higher or lower expression level, despite a normal DNA copy number. The protein expression level was consistent with that of mRNA, and in cell lines with a higher expression level, MET was constitutively activated. Notably, the expression level of *MET* was significantly higher in patients who died ($P = 0.02$), in patients with stage IV ($P = 0.04$), as well as in patients with *PAX3-FKHR* chimeric transcript ($P = 0.04$). On the other hand, reduced or absent expression of $p16^{INK4A}$ and/or $p14^{ARF}$ showed no significant correlation with the clinicopathological parameters, except for the age at diagnosis. Our data suggest that MET plays a role in the progression of RMS.

INTRODUCTION

Rhabdomyosarcoma (RMS) is a heterogeneous group of malignant tumors of mesenchymal origin and is thought to arise from cells committed to the skeletal muscle lineage. RMS is the most common soft-tissue sarcoma in children, with an annual incidence of 4–7 per million of 15 years of age or younger, and is also the third most common extracranial solid tumor of childhood (Dagher and Helman, 1999; Merlino and Helman, 1999). Approximately 65% of cases are diagnosed in children less than 6 years of age with remaining cases noted in the 10–18-year-old age group. RMS falls into the broader category of small blue, round cell tumors of childhood, and is subdivided into two major histological subtypes, embryonal rhabdomyosarcoma (ERMS) and alveolar rhabdomyosarcoma (ARMS). ERMSs are typically comprised of spindle shaped cells, with a stromal rich appearance. In general, embryonal tumors tend to occur in the younger age group and occur more frequently in the head and neck region and less frequently in the extremities. Approximately two thirds of all RMSs are of embryonal histology. ARMSs are typically comprised of small round densely packed cells, arranged around spaces resembling pulmonary alveoli. Alveolar tumors tend to occur in the older age group and are more frequently seen in extremity lesions. A number of molecular/genetic lesions have been associated with RMS. Embryonal tumors are characterized by loss of heterozygosity (LOH) at the 11p15 locus, a region harboring a

Supported by: A Grant-in-Aid for Cancer Research; Research on Children and Families from Ministry of Health, Labor and Welfare of Japan; Ministry of Education, Culture, Sports, Science and Technology of Japan.

*Correspondence to: Yasuhide Hayashi, MD, Director, Gunma Children's Medical Center, 779 Shimohakoda, Hokkitsu, Shibukawa, Gunma 377-8577, Japan.
E-mail: hayashiy-tky@umin.ac.jp

Received 22 June 2006; Accepted 21 November 2006
DOI 10.1002/gcc.20416
Published online 22 January 2007 in Wiley InterScience (www.interscience.wiley.com).

number of genes implicated in oncogenesis, such as the insulin-like growth factor 2 (*IGF2*) gene, and associated with alterations of imprinting. In contrast to ERMS, ~70–80% of ARMS carry a characteristic chromosomal translocation juxtaposing the 5′ DNA-binding domains of *PAX3* or *PAX7*, members of the Paired Box transcription factor family, to the transactivation domain at the 3′ portion of *FOXO1A* (forkhead box O1A, also *FKHR*), a member of the forkhead/HNF-3 transcription factor family, which results in two fusion genes, t(2;13)(q35;q14) (*PAX3-FOXO1A*) in most cases, and t(1;13)(p36;q14) (*PAX7-FOXO1A*) at a less frequency (Dagher and Helman, 1999; Merlino and Helman, 1999; Sorensen et al., 2002). It has been reported that ARMS is associated with a poor prognosis (Crist et al., 1990; Newton et al., 1995). Despite aggressive treatment including surgery, dose-intensive combination chemotherapy, and radiation therapy, the outcome for patients with metastatic tumors remains poor.

RMS has been thought to arise as a consequence of regulatory disruption of skeletal muscle progenitor cell growth and differentiation. The delicate balance between proliferation and differentiation is normally regulated in large part through the action of a multitude of growth factors, whose signals are transmitted by members of the MyoD family of helix-loop-helix proteins, and key regulatory cell cycle factors (Merlino and Helman, 1999). *PAX3* is important for regulation of myogenesis by activating transcription of several target genes such as *MyoD* and *MET* (Epstein et al., 1996; Buckingham et al., 2003). The *MET* proto-oncogene encodes a receptor tyrosine kinase that mediates the multifunctional and potentially oncogenic activities of hepatocyte growth factor/scatter factor (HGF/SF), including the promotion of cellular growth, motility and survival, extracellular matrix degradation, and angiogenesis (Jeffers et al., 1996; Matsumoto and Nakamura, 1996; Trusolino and Comoglio, 2002). MET is essential in the migration of myogenic precursor cells into the limb bud and *Met* knockout mice have no limb muscles (Bladt et al., 1995). *MET* activity is deregulated by genetic mutations, gene amplification, protein overexpression and/or the creation of HGF/SF-MET autocrine loops, which have been implicated in the development and progression of a wide variety of human cancers, such as papillary renal-cell carcinoma (Schmidt et al., 1997), breast carcinoma (Tuck et al., 1996), hepatocellular carcinoma (Takeo et al., 2001), as well as osteosarcoma (Ferracini et al., 1995). It has also been reported in a previous study that *MET* is aberrantly expressed in RMS (Ferracini et al., 1996). On the other hand, cyclin-dependent kinase inhibitor 2A (*CDKN2A*) has been identified as a suppressor of numerous human hematological malignancies and solid tumors (Sherr, 2001). The *CDKN2A* gene is remarkable in that it has alternative reading frames resulting in two tumor suppressor genes, $p16^{INK4A}$ and $p14^{ARF}$, encoding two unrelated proteins (Robertson and Jones, 1999). $p16^{INK4A}$ and $p14^{ARF}$, acting through the downstream retinoblastoma protein (RB1) and TP53, respectively, help regulate cellular transit through the cell cycle as well as senescence and apoptosis (Zhang et al., 1998). It has been shown that forced expression of cyclin D1 inhibited the ability of *MyoD* to transactivate muscle-specific genes and correlated with phosphorylation of MyoD, whereas transfection of myoblasts with cyclin-dependent kinase (Cdk) inhibitors *p21* and $p16^{INK4A}$ augmented muscle-specific gene expression in cells (Skapek et al., 1995). Recently, it was found that RMS was induced with extremely high penetrance by the simultaneous loss of *Ink4a/Arf* function and disruption of Met signaling in $Ink4a/Arf^{-/-}$ mice transgenic for *HGF/SF* (Sharp et al., 2002). It has also been reported that *Met* is necessary for *Pax3-Foxo1a*-mediated effect in mice, and *Met* had a role in both alveolar and embryonal RMS maintenance (Taulli et al., 2006). Furthermore, although it was shown that *Pax3-Foxo1a* was insufficient to cause tumors in knock-in mice (Lagutina et al., 2002; Keller et al., 2004b), *Pax3-Foxo1a* homozygosity with accompanying Ink4a/Arf or Tp53 pathway disruption substantially increases the frequency of alveolar RMS tumor formation in mice (Keller et al., 2004a).

To clarify whether *MET* and *CDKN2A*, situated at the nexus of pathways regulating myogenic growth and differentiation, represent critical targets in RMS, we performed mutational and expression analyses for *MET* and *CDKN2A*, and evaluated the relationship between the expression levels of these genes and the clinicopathological parameters.

MATERIALS AND METHODS

Cell Lines, Primary Tumors, and Normal Controls

Seven RMS cell lines (SJRH-1, SJRH-4, SJRH-18, SJRH-30, RD, RMS, SCMC-RM2) were examined in this study (Uno et al., 2002). Cell lines SJRH-4, SJRH-18, SJRH-30, and SCMC-RM2 are alveolar type, whereas the others are embryonal type. All of the cell lines were cultured in RPMI 1640 medium (GIBCO, Invitrogen, Tokyo, Japan)

TABLE 1. Primers for the *MET*, $p16^{INK4A}$, and $p14^{ARF}$ Genes for PCR-SSCP.

Exon	Primer sequence (5′→3′) Forward	Reverse
MET[a]		
14	CCATGATAGCCGTCTTTAAC	ATACTTACTTGGCAGAGGT
15	GTCCCCATTAAATGAGGTTT	ATCTGCAAAGGCCAAAGATA
16	ATGTTACGCAGTGCTAACC	GTAGCTGATTTTTCCACAAG
17	GAAGTTAATGTCTCCACCAC	TGGCTTACAGCTAGTTTGCC
18	TTCTAACTCTCTTTGACTGC	CAGATTCCTCCTTGTCACTT
19	ATTCTATTTCAGCCACGGG	AGGAGAAACTCAGAGATAACC
20	ACCTCATCTGTCCTGTTTC	CCAAAAAGAAAGACATGCTG
21	GGGTCTCTTACAGCATGTCT	GTGTGGACTGTTGCTTTGAC
$p16^{b}$		
1	GCTGCGGAGAGGGGGAGAGCAGGCA	CTGCAAACTTCGTCCTCCA
2-1	CTTCCTTTCCGTCATGCCG	CTCAGCCAGGTCCACGGGCA
2-2	TTCCTGGACACGCTGGTGGTG	GGAAGCTCTCAGGGTACAAA
3	TGCCACACATCTTTGACCTC	AAAACTACGAAAGCGGGGTG
$p14^{b}$		
1-1	CGCTCAGGGAAGGCGGGTGC	AACCACGAAAACCCTCACTC
1-2	ATGGTGCGCAGGTTCTTGGT	ACCAAACAAAACAAGTGCCG

[a]GenBank accession number for *MET* is NT_007933.
[b]GenBank accession number for *CDKN2A* is NT_008413.

supplemented with 10% fetal bovine serum in a humidified atmosphere containing 5% CO_2 at 37°C.

Thirty-two primary RMS tumors, obtained at the time of initial surgery or biopsy in several hospitals in Japan (1993–2005), were examined. Histopathological diagnosis was made by pathologists at each hospital. Of the 32 cases (age range, 0–20 years; median age, 5.8 years), 5 were classified as stage I, 5 as II, 10 as III, and 12 as IV, according to the Intergroup Rhabdomyosarcoma Study-IV (IRS-IV) staging classification. Twenty-one cases were ERMS, and 11 were ARMS. Patients with stage I or II were treated with surgery alone or surgery plus chemotherapy, mainly vincristine. Patients with stage III or IV were treated with surgery, radiotherapy, intensive multidrug chemotherapy, and if necessary, autologous bone marrow transplantation.

All of the cell lines and fresh tumors were previously screened for mutations of *TP53*.

Normal human skeletal muscle total RNA was obtained from two healthy patients (aged 3 and 5). Ten peripheral blood (PB) samples from healthy volunteers were also used as normal controls.

Informed consent was obtained from the patients and/or their parents as well as healthy volunteers.

DNA and RNA Preparation

High-molecular-weight DNA was extracted from all samples by proteinase K digestion and phenol/chloroform extraction. Total RNA was extracted from all of the cell lines and 17 fresh tumors using the acid guanidine thiocyanate-phenol chloroform method. Randomly primed cDNA was synthesized from total RNA using a cDNA synthesis kit as previously described (Shibuya et al., 2001).

Mutational Analyses for *MET* and *CDKN2A* in RMS

The mutations of *MET* identified to date are clustered in the transmembrane domain and tyrosine kinase domain (Trusolino and Comoglio, 2002). Therefore, we examined exons 14–21 of *MET*, which encompassed the two domains and the juxtamembrane region, for all of the cell lines and fresh tumors by PCR-single-strand conformation polymorphism (PCR-SSCP) analyses as described elsewhere (Chen et al., 2005). For *CDKN2A*, we screened its whole coding region by PCR-SSCP. The primers for PCR-SSCP are listed in Table 1. For samples that showed altered mobility, we subjected the PCR products to direct sequencing analyses (Chen et al., 2005, 2006). Furthermore, we performed another round of direct sequence analyses in all cell lines for *MET* and *CDKN2A* to verify the results of PCR-SSCP.

Real-Time Quantitative PCR

For seven RMS cell lines and 17 fresh tumors, real-time quantitative PCR (RQ-PCR) analyses were carried out to quantify the expression levels of *MET*, $p16^{INK4A}$ and $p14^{ARF}$, using a QuantiTect™ SYBR Green PCR Kit (Qiagen, Tokyo,

Japan) with an iCycler iQ™ real-time PCR detection system (Bio-Rad Japan, Tokyo, Japan). The reaction mixture was prepared as follows: 1 μl of cDNA, 1×QuantiTect SYBR Green PCR Master Mix, 0.3 μm of each primer and 0.5 U of uracil-*N*-glycosylase (Applied Biosystems, Tokyo, Japan) in a final volume of 50 μl. The amplification conditions for quantitation were an initial 2 min of incubation at 50°C, 15 min at 95°C, followed by 40 cycles of amplification (denaturation at 95°C for 30 sec, annealing at the respective temperatures for 30 sec, extension at 72°C for 30 sec) (Chen et al., 2003). The primer sets used for real-time quantitative reverse transcriptase-PCR were as follows: sense 5′-GGTTGCTGATTTTGGTCTTG-3′ and antisense 5′-GCAGTATTCGGGTTGTAGGA-3′ for *MET* (GenBank accession number NM_000245); sense 5′-GCCCAACGCACCGAATAG-3′ for $p16^{INK4A}$ (GenBank accession number NM_058197), 5′-TCTGGTTCTTTCAATCGGGGA-3′ for $p14^{ARF}$ (GenBank accession number NM_058195) and the same antisense 5′-ACCACCAGCGTGTCCAGGAA-3′ for $p16^{INK4A}$ or $p14^{ARF}$. The β-*actin* gene served as an endogenous control. The primers for β-*actin* amplification were sense 5′-CTTCTACAATGAGCTGCGTG-3′ and antisense 5′-TCATGAGGTAGTCAGTCAGG-3′. For the purpose of normalization, the relative expression level was calculated by dividing the expression level of the respective gene by that of the β-*actin* gene for each sample.

For the seven RMS cell lines and 17 fresh tumors, the relative DNA copy number of *MET* or *CDKN2A* in each sample was quantified using RQ-PCR analyses similar to above. Each DNA sample had an $A_{260/280}$ ratio in the range 1.60–1.80 and was diluted to 100 ng/μl before use. The primer set for *MET* was that for mutational screening of exon 16 and the primer set for *CDKN2A* was that for mutational screening of the common exon 2, respectively (Table 1). The *B2M* (β-2-microglobulin) gene, which was a housekeeping gene on chromosome 15q21-q22.2 (Lillington et al., 2002), was used as an endogenous reference and the copy number of *MET* as well as *CDKN2A* in each sample was normalized by the corresponding *B2M* value. The primers for *B2M* amplification were sense 5′-AAGTGGAGCATTCAGACTTG-3′ and antisense 5′-TCCCTGACAATCCCAATATG-3′ (GenBank accession number NT_010194).

All of the reactions were run in triplicate. The primers used for RT-PCR were designed to prevent DNA amplification, and the melting curve was incorporated to detect whether primer dimers or other undesired products were amplified. In addition, all of the amplified products were subjected to gel electrophoresis, and if necessary, direct sequence analysis was performed to confirm the expected PCR products.

Detection of *PAX3-FKHR* and *PAX7-FKHR* Chimeric Transcripts

For the seven RMS cell lines and 17 fresh tumors, we also examined the expression of *PAX3-FKHR* and *PAX7-FKHR* chimeric transcripts as described previously (Galili et al., 1993; Davis et al., 1994).

Western Blotting and Immunoprecipitation Analyses

Rabbit polyclonal antibodies against human MET (C-12) and mouse monoclonal antibodies against phosphorylated tyrosine (p-Tyr) (PY99) were purchased from Santa Cruz Biotechnology (Santa Cruz, CA). The secondary antibodies (donkey anti-rabbit IgG and sheep anti-mouse IgG conjugated with horseradish peroxidase) and enhanced chemiluminescence reagent were purchased form Amersham Biosciences (Piscataway, NJ). Total cellular proteins were extracted by lysing 1×10^6 cells with a lysis buffer [50 mM HEPES-NaOH (pH7.0), 1% NP40, 1% sodium deoxycholate, 0.1% sodium dodecyl sulfate (SDS), 250 mM NaCl, 5 mM NaF, 1 mM DTT, 1 mM phenylmethylsulfonyl fluoride, and 50 μg/ml aprotinin] from 7 RMS cell lines (Takita et al., 1997). The proteins were separated by SDS-PAGE by loading the lysates containing 50 μg of total protein on a 4–20% gradient gel, and then transferring onto a polyvinylidene difluoride transfer membrane (Millipore, Billerica, MA) (Takita et al., 1997). The membranes were incubated with the anti-MET antibody, followed by the HRP-conjugated secondary antibody. The resultant immunoproducts were detected with the ECL Western Blotting Analysis System. Equal protein loading was confirmed by staining the membrane with Coomassie brilliant blue. The Western blotting analysis for MET was performed three times, then the blots were scanned, and the level of MET in each sample was estimated using the NIH Image 1.61 software (Wayne Rasband, National Institutes of Health, MD). The protein expression level of each cell line was calculated as mean ± SD.

For immunoprecipitation (IP), lysates containing 500 μg of total protein were pretreated with 1 μg of normal rabbit IgG and 20 μl of protein G-plus

TABLE 2. Expression of *MET*, $p16^{INK4A}/p14^{ARF}$, and *PAX3-FOXO1A* Transcript, and Mutations of *TP53* in RMS Cell Lines

		MET		*p16*	*p14*		
Cell lines	Histology	mRNA[a]	Protein[a]	mRNA	mRNA	*PAX3-FOXO1A*	Mutation of *TP53*
SJRH-1	E	13.06 ± 0.50	11.78 ± 8.08	0.03 ± 0.00	0.74 ± 0.12	−	Tyr220Cys
SJRH-4	A	122.99 ± 30.86	71.35 ± 37.72	0.73 ± 0.02	0.96 ± 0.22	+	13bp del[b]
SJRH-18	A	59.70 ± 13.07	60.12 ± 21.94	0.13 ± 0.08	0.38 ± 0.11	+	Gly187Cys
SJRH-30	A	363.04 ± 54.41	166.35 ± 61.83	0.92 ± 0.01	1.19 ± 0.02	+	Tyr205Cys
RD	E	28.13 ± 7.14	22.45 ± 7.05	0.16 ± 0.03	0.90 ± 0.04	−	Arg248Trp
RMS	E	8.17 ± 0.74	14.66 ± 6.61	0.49 ± 0.07	0.97 ± 0.03	−	Arg282Trp[c]
SCMC-RM2	A	155.08 ± 29.28	109.50 ± 62.99	0.55 ± 0.03	1.05 ± 0.07	+	−

E, embryonal type; A, alveolar type.
[a]The values for mRNA and protein indicate mean ± SD.
[b]Nucleotide 701–713 (GenBank accession number for *TP53* is NM_000546).
[c]Single nucleotide polymorphism (SNP). GenBank accession number for Arg282Trp is rs28934574.

agarose beads (Santa Cruz, CA) at 4°C for 30 min. After removal of the beads by centrifugation, lysates were incubated with the anti-MET antibody (2 μg) and 20 μl of protein G-plus agarose beads overnight at 4°C. The immunoprecipitates were washed three times with PBS/0.1%NP-40 and resuspended in lysis buffer, followed by Western blot analyses as described above with anti-p-Tyr (PY99). Then, the antibodies were stripped from the membrane in a stripping buffer containing 62.5 mmol/l Tris, 2% SDS, and 100 mmol/l β-mercaptoethanol. The membrane was reprobed with C-12 and the relative secondary antibodies to confirm the expression of MET.

Statistical Analyses

The Mann-Whitney *U* test was used to compare the expression level of each gene between subgroups of RMS. Fisher's exact test was used to evaluate the statistical significance of differences in proportions among groups. Kaplan–Meier survival plots were constructed, and log-rank tests were used to estimate survival. Exact 95% CI of proportions were calculated on the basis of binomial distribution. The Spearman rank correlation was calculated to evaluate the correlation between the mRNA expression and protein expression of MET. Two-sided $P < 0.05$ was required for significance. All analyses were carried out with StatView-J 4.5software (Abacus Concepts, CA).

RESULTS

Mutations of *MET* and *CDKN2A* in RMS

For seven cell lines and 32 fresh tumors of RMS, no mutations (0.0%; 95% CI, 0.0–9.0%) were detected in exons 14–21 of *MET* by PCR-SSCP. For *CDKN2A*, one nonsense mutation (CGA > TGA) (2.6%; 95% CI, 0.5–13.2%), resulting in a truncated protein at codon 80 of $p16^{INK4A}$, was observed in an ARMS cell line, SJRH-18. The same mutation was reported previously in melanoma (Orlow et al., 2001). This C > T transition also results in a missense mutation (Pro135Leu) in $p14^{ARF}$. A polymorphism (Ala148Thr) in $p16^{INK4A}$ was detected in another ARMS cell line, SJRH-30. No mutations of $p16^{INK4A}$ or $p14^{ARF}$ were identified in the 32 fresh tumors.

Expression of *MET* and $p16^{INK4A}/p14^{ARF}$ mRNA in RMS

Using RQ-PCR, the expression of *MET* was detected in all of the RMS samples and normal skeletal muscles. The *MET*/β-*actin* value in RMS ranged from 6.16 to 424.42, with a mean value of 102.60 ± 124.86, whereas the *MET*/β-*actin* value in normal muscles was 33.20 ± 3.77. Overexpression of *MET* (> mean value), was detected in 7 of 24 RMS samples, which included 3 alveolar cell lines (SJRH-4, SJRH-30, SCMC-RM2) (3/7), and 2 alveolar and 2 embryonal type tumors (4/17) (Table 2 and Fig. 1A).

The $p16^{INK4A}$/*β-actin* value in RMS ranged from 0 to 3.59, with a mean value of 0.74 ± 0.96. Reduced or absent expression of $p16^{INK4A}$ ($p16^{INK4A}$/β-*actin* less than half the mean value) was observed in 11 of 24 samples, which included 3 cell lines (SJRH-1, SJRH-18, RD) and 8 fresh tumors (Table 2).

The $p14^{ARF}$/*β-actin* value in RMS ranged from 0 to 3.53, with a mean value of 0.85 ± 0.94. Reduced or absent expression of $p14^{ARF}$ ($p14^{ARF}$/*β-actin* less than half the mean value) was shown in 10 of 24 samples, which included 1 cell line (SJRH-18) and 9 fresh tumors (Table 2).

Two fresh tumors (2/24) with overexpression of *MET* had also concomitant reduced or absent expression of $p16^{INK4A}$ and/or $p14^{ARF}$; 1 was an ERMS and the other was an ARMS.

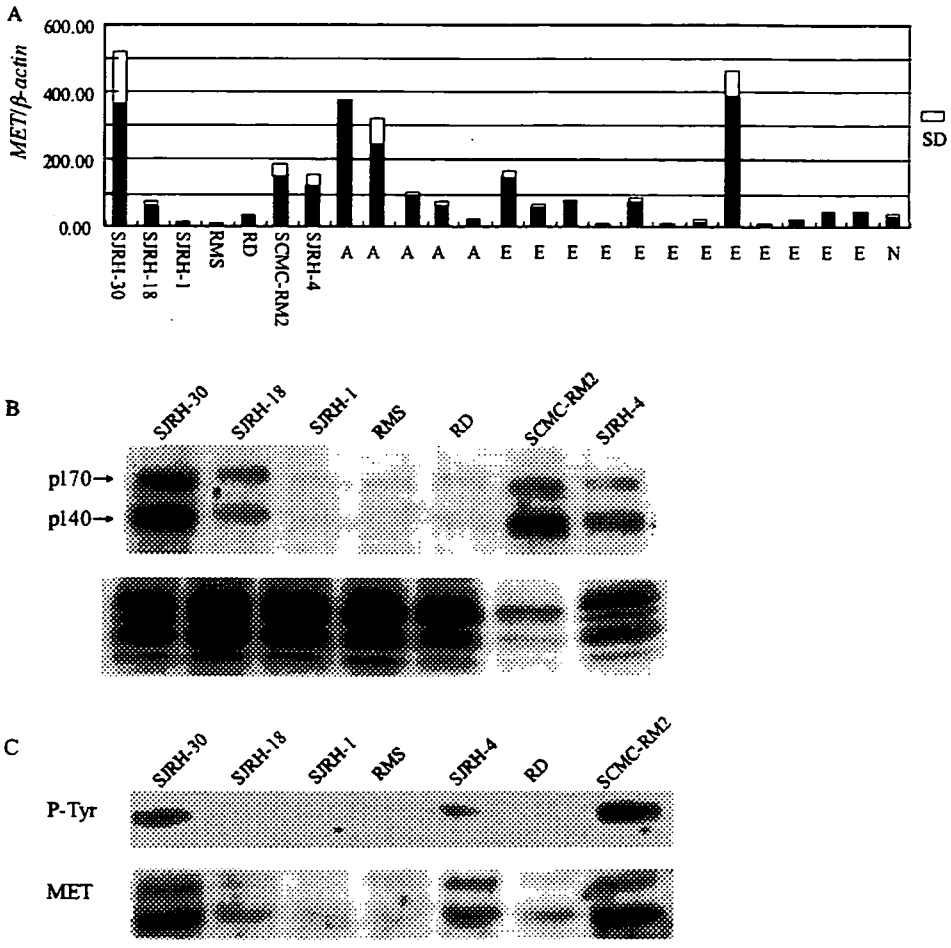

Figure 1. Expression of MET mRNA and protein in RMS. (A) Expression of *MET* mRNA (*MET/β-actin*) in RMS cell lines and fresh tumors as well as normal skeletal muscles detected by real-time quantitative RT-PCR. A, alveolar; E, embryonal; N, normal skeletal muscle; SD, SD. (B) Western blotting for MET in seven RMS cell lines. The arrows indicate the 170 kDa precursor and 140 kDa β-subunit, respectively. In the bottom panel, the loading of protein was shown by protein staining with Coomassie brilliant blue. (C) Tyrosine phosphorylation of MET in RMS cell lines detected by immunoprecipitation. As a control, the membrane was stripped and reprobed with anti-MET antibody, which was shown in the bottom panel.

Expression and Activation of MET Protein in RMS Cell Lines

To determine whether the expression of MET protein correlates with that of *MET* mRNA, Western blot analysis was carried out for the seven RMS cell lines. As shown in Figure 1B, a higher expression of MET protein with a mass of 140 kDa as well as a mass of 170 kDa, represented the β-subunit and precursor of MET respectively (Giordano et al., 1989), was detected in SJRH-4, SJRH-18, SJRH-30, and SCMC-RM2, consistent with the higher expression level of mRNA in these cell lines. In comparison, a relatively weak expression of p140 and p170 was detected in SJRH-1, RD and RMS, which showed a lower expression level of *MET* by RQ-PCR. The density of p140 ranged from 11.78 to 166.35 and with an average of 65.17 ± 57.00 (Table 2). The mRNA expression level of *MET* in each cell line, as detected by RQ-PCR, showed a significant correlation with the density of p140 (correlation coefficient: 0.964; $P = 0.018$).

We further studied the activation status of the MET receptor in these cell lines by immunoprecipitation analysis. As shown in Figure 1C, a band of phosphorylated MET was observed in SJRH-4, SJRH-30, and SCMC-RM2, indicating the constitutive activation of MET in these cells.

Relative DNA Copy Number of *MET* and *CDKN2A* in RMS

The relative DNA copy number of *MET* (calculated as *MET/B2M*) in the seven cell lines and 17 fresh tumors ranged from 0.60 to 1.71 with an average of 0.96 ± 0.36. No samples showed more than twice the average of the relative DNA copy

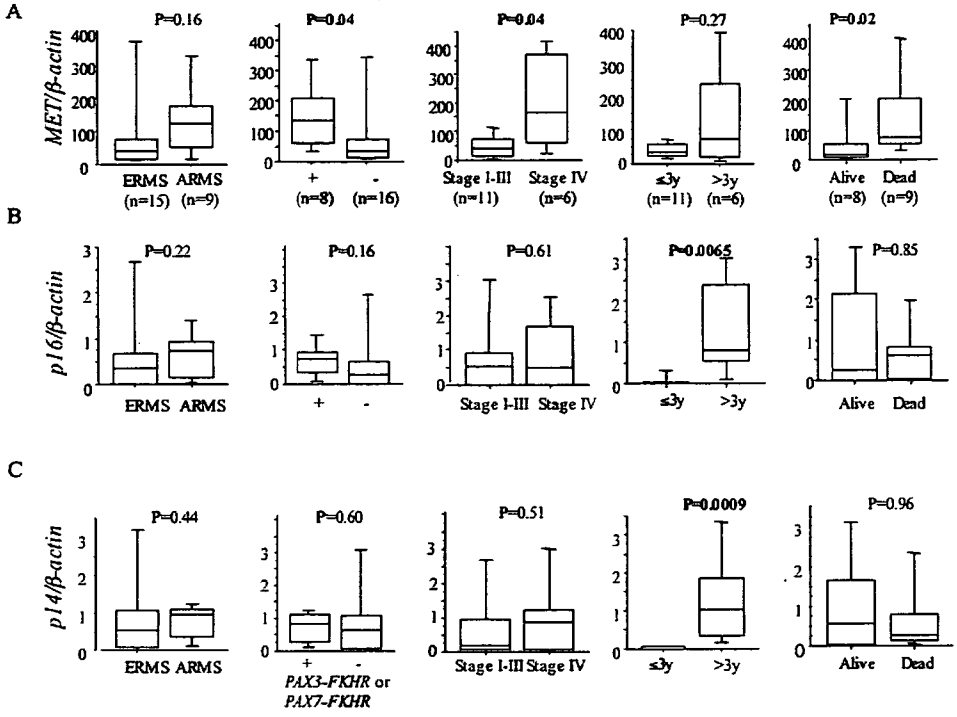

Figure 2. The relationship between clinicopathological parameters and mRNA expression of the genes *MET* (A), $p16^{INK4A}$ (B), and $p14^{ARF}$ (C). The expression levels of each gene were compared among groups classified by histology (including cell lines), *PAX3-FOXO1A* or *PAX7-FOXO1A* transcript expression (including cell lines), stage, age at diagnosis, as well as outcome using Mann-Whitney *U* test. It was shown in bold when $P < 0.05$.

number detected in normal skeletal muscle (1.14) or in normal PB (1.22).

The relative DNA copy number of *CDKN2A* (calculated as *CDKN2A/B2M*) was also evaluated in the 24 samples. The mean value of *CDKN2A/B2M* was 0.73 ± 0.43 with a range from 0.24 to 1.44. Three cell lines (SJRH-4, RD, RMS) (3/7) and two fresh tumors (2/17) showed less than half the mean value of the relative DNA copy number.

Expression of *PAX3-FOXO1A* and *PAX7-FOXO1A* Chimeric Transcripts in RMS

The *PAX3-FOXO1A* chimeric transcript was detected in 4 of 4 alveolar type cell lines (SJRH-4, SJRH-18, SJRH-30 and SCMC-RM2) (Table 2). There were five ARMSs among the 17 fresh tumors; 3 having *PAX3-FOXO1A* and 1 having *PAX7-FOXO1A* (4/5). Of the 4 alveolar type cell lines with expression of *PAX3-FOXO1A*, 3 showed overexpression of *MET* and of the 3 ARMSs having *PAX3-FOXO1A*, 2 showed overexpression of *MET*. The sample having *PAX7-FOXO1A* showed an expression level of *MET*/β-*actin* at 21.37 ± 1.04.

Mutations of *TP53* in RMS

The mutations of *TP53* were detected in 5/7 cell lines and 3/17 fresh tumors. The mutations in five cell lines included four missense mutations (Gly187Cys, Tyr205Cys, Tyr220Cys, and Arg248Trp) and a 13 bp deletion (nucleotides 701–713) in exon 5, which resulted in a truncated transcript (Table 2). In the five cell lines having mutations of *TP53*, two showed overexpression of *MET*. The three fresh tumors having mutations of *TP53* included an insertion of 6 bp (ACTACA) between nucleotides 960 and 961 in an ERMS (GenBank accession number: NM_000546), a missense mutation (Asp49His) in an ERMS, and a nonsense mutation (Arg → stop codon) at codon 342 in the ARMS with *PAX7-FOXO1A*. Overexpression of *MET* was only detected in one of the three samples having mutations of *TP53*.

Relationship Between the Expression Level of *MET* or $p16^{INK4A}/p14^{ARF}$ and Clinicopathological Parameters in RMS

To address the relationship between the clinicopathological parameters and the expression levels of *MET* and $p16^{INK4A}/p14^{ARF}$, we compared the expression level of each gene between groups classified by patients' age, stage, histology, *PAX3-FOXO1A* or *PAX7-FOXO1A* transcript expression, as well as outcome (Fig. 2). By nonparametric

Mann-Whitney *U* test, we found that the patients with stage IV showed higher expression of *MET* than those with stage I–III ($P = 0.04$). Furthermore, the expression level of *MET* was significantly higher in the patients who died of cancer than those who were alive ($P = 0.02$). In all samples including cell lines, the group with *PAX3-FOXO1A* or *PAX7-FOXO1A* transcript showed higher expression of *MET* than that without such transcripts ($P = 0.04$). There was no statistical significance between the groups classified by histology ($P = 0.16$) and age ($P = 0.27$), although a tendency of higher expression of *MET* was shown in ARMS as well as in patients over 3 years old (Fig. 2A). Using the median expression level (58.30) as a cutoff, we also compared the difference in proportions among groups by Fisher's exact test. In all samples, overexpression of *MET* (>58.30) was detected in 7 of 9 ARMSs compared with that in 5 of 15 ERMSs ($P = 0.05$), as well as in 7 of 8 samples with *PAX3-FOXO1A* or *PAX7-FOXO1A* transcripts compared with that in 5 of 16 samples without such transcripts ($P = 0.03$). In fresh tumors, overexpression of *MET* was shown in 7 of 9 patients who died of cancer but only in 1 of 8 patients who survived ($P = 0.03$), as well as in 5 of 6 patients with stage IV compared with 3 of 11 patients with stage I–III ($P = 0.05$). The survival curve on Kaplan-Meier analyses showed that higher expression of *MET* correlated with poorer survival ($P = 0.05$, log-rank test) (Fig. 3).

On the other hand, significantly lower expression levels of $p16^{INK4A}$ and $p14^{ARF}$ were found in patients younger than 3 years ($P = 0.0065$ and $P = 0.0009$, respectively); however, the expression levels of $p16^{INK4A}$ and $p14^{ARF}$ showed no significant difference between groups classified by stage, histology, expression of *PAX3-FOXO1A* or *PAX7-FOXO1A* transcript, or prognosis (Mann-Whitney *U* test; Figs. 2B and 2C).

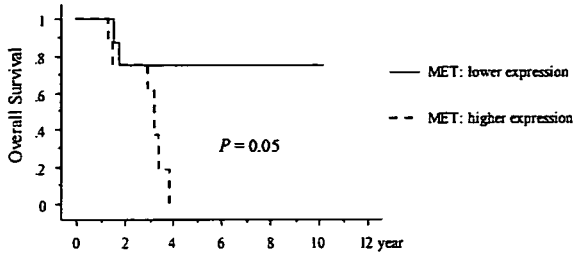

Figure 3. Kaplan-Meier curve for overall survival rates of patients with higher (>median) or lower expression (≤median) of *MET*. *P* value was calculated by log-rank test.

DISCUSSION

It has been reported that HGF/SF-MET signals induce proliferative and antiapoptotic responses in various cell types (Trusolino and Comoglio, 2002; Birchmeier et al., 2003). Analyses of HGF/SF and Met in mice have shown their essential regulatory role in development, such as the growth and survival of epithelial cells and migration of myogenic precursor cells (Bladt et al., 1995; Schmidt et al., 1995; Uehara et al., 1995). Upregulation of MET and HGF/SF expression is observed in several injured tissues, whereas deregulation of MET and HGF/SF signaling has emerged as a crucial feature of many human malignancies. For instance, germline or somatic activating mutations in the tyrosine kinase domain of *MET* have been demonstrated in papillary renal carcinomas (Schmidt et al., 1997), in childhood hepatocellular cancer (Park et al., 1999), and in metastases of carcinoma (Lorenzato et al., 2002). Overexpression and/or amplification of *MET* with autocrine or paracrine loop have been noted in carcinomas of breast (Tuck et al., 1996), thyroid (Di Renzo et al., 1992), and pancreas (Di Renzo et al., 1995), as well as in sarcomas, such as osteosarcoma (Ferracini et al., 1995) and RMS (Ferracini et al., 1996). Characterization of MET and HGF/SF activities in proliferation, invasion, angiogenesis, and antiapoptosis delineates the stages at which these molecules participate in tumor progression (Birchmeier et al., 2003). Furthermore, a number of studies have shown that HGF/SF and/or MET over- or misexpression often correlates with poor prognosis in many malignancies (Birchmeier et al., 2003). It is also reported that Pax3 modulates the expression of *Met* during limb muscle development by mediating the migration of myogenic precursor cells into the limb anlage (Bladt et al., 1995; Epstein et al., 1996), while the expression of *MET* is repressed in differentiated myotubes and in adult nondividing muscle cells (Sonnenberg et al., 1993). The *PAX3-FOXO1A* fusion protein upregulates the expression of *MET* in alveolar type RMS (Ginsberg et al., 1998).

In this study, we detected the expression of *MET* in all of the RMS samples by RQ-PCR and the expression levels showed a large variety among samples. This is comparable to an early report that the expression of *MET* was detected in 6 of 6 RMS cell lines and 9 of 14 RMS fresh tumors by Western blot analysis (Ferracini et al., 1996). In their study, cell lines RD and SJRH-30 with a higher expression of MET also showed amplification of *MET* on Southern blot analysis, whereas SJRH-1 and SJRH-4 with a relatively lower expression level showed no amplification. We found that the expression level of

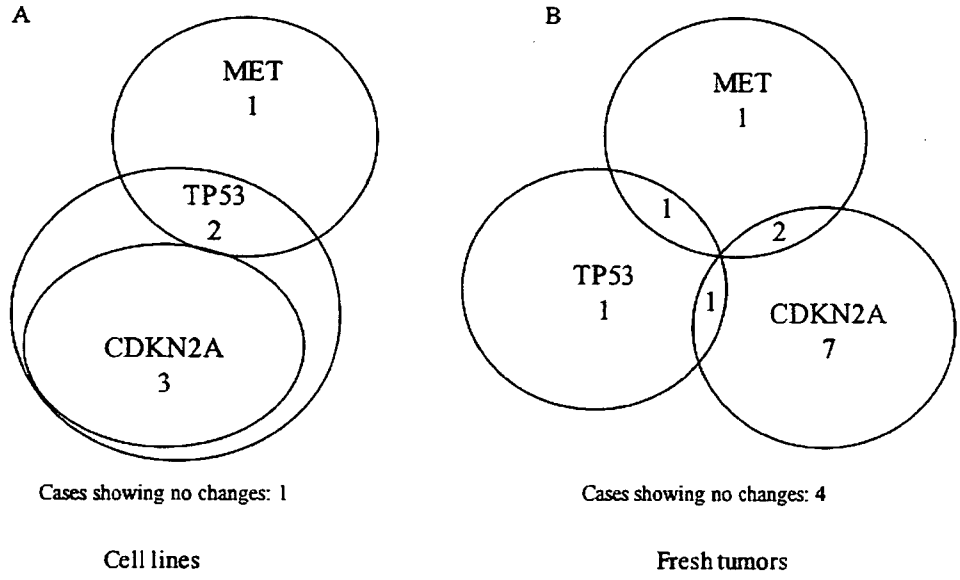

Figure 4. The distributions of overexpression of *MET* (> mean value), reduced or absent expression of $p16^{INK4A}$ and $p14^{ARF}$ (< half the mean value), and the mutations of *TP53* in seven cell lines (A) and 17 fresh tumors (B).

MET is higher in ARMS cell lines SJRH-4, SJRH-18, SCMC-RM2, and SJRH-30 than in ERMS cell lines SJRH-1, RMS, and RD by RQ-PCR (Fig. 1A). These results were also consistent with the results of Western blotting for MET protein expression. Furthermore, immunoprecipitation analysis showed constitutive tyrosine phosphorylation of MET in SJRH-4, SJRH-30, and SCMC-RM2, which indicated an autocrine manner. There was no obvious change of the relative DNA copy number observed by RQ-PCR and no mutations detected by PCR-SSCP in all samples. Thus, our results indicated that overexpression of *MET* in RMS was probably not induced by amplification/hyperploidy and that mutations of *MET* may not be of major pathogenetic importance in RMS.

Our data also showed a significantly higher expression level of *MET* in patients who died of cancer than in patients who were alive. The higher expression level was also observed in patients with stage IV as well as in patients with chimeric transcripts. A tendency toward higher *MET* expression was observed in ARMS as well as in patients over 3 years of age. Similar results were obtained when using the median level as a cutoff for *MET* expression. The survival curve on Kaplan-Meier analyses further confirmed that the expression level of *MET* correlates with the outcome of RMS patients. In RMS, it has previously been shown that older age at diagnosis, advanced stage, alveolar type, and expression of *PAX3-FOXO1A* are associated with poor prognosis (Crist et al., 1990; Newton et al., 1995; Sorensen et al., 2002). Earlier studies have also suggested that HGF/SF stimulates transmigration and invasiveness of RMS cells in vitro (Ferracini et al., 1996). It has also been reported recently that Met is necessary for a *Pax3-Foxo1a*-mediated effect in mice, and that Met has a role in RMS maintenance (Taulli et al., 2006). Taken together, it seems that MET may play an important role in the progression of RMS. A larger panel of samples should be studied to confirm this.

The *CDKN2A* gene encodes two unrelated proteins that function in tumor suppression. $p16^{INK4A}$ binds to and inhibits the activity of CDK4 and CDK6, and $p14^{ARF}$ promotes MDM2 (transformed 3T3 cell double min 2, TP53 binding protein) degradation and arrests the cell cycle in a TP53-dependent manner (Zhang et al., 1998). Thus, deletion of the *CDKN2A* locus simultaneously impairs both INK4A-cyclinD/CDK4-RB and ARF-MDM2-TP53 pathways. Mutations, homozygous deletions and altered expression of *CDKN2A* have been discovered in a wide range of human solid tumors as well as hematological malignancies (Kamb et al., 1994; Okamoto et al., 1994; Ohnishi et al., 1995; Takita et al., 2004). There has been some controversy about the significance of $p16^{INK4A}/p14^{ARF}$ in predicting the prognosis of malignancies such as neuroblastoma (Takita et al., 1998; Omura-Minamisawa et al., 2001) and childhood acute lymphoblastic leukemia (Mekki et al., 1999; Dalle et al., 2002). The association of $p16^{INK4A}$ and $p14^{ARF}$ expression with prognosis in RMS has not been well docu-

mented. In this study, we identified a nonsense mutation at codon 80 of $p16^{INK4A}$ in one cell line, SJRH-18, resulting in reduced expression of both $p16^{INK4A}$ and $p14^{ARF}$. This result is consistent with an early report showing that *CDKN2A* mutations are rare in RMS (Iolascon et al., 1996). No significant correlation was shown between the reduced or absent expression of $p16^{INK4A}$ and $p14^{ARF}$ and the clinicopathological factors, except for patients' age, which showed that the expression levels of $p16^{INK4A}$ and $p14^{ARF}$ were significantly lower in patients younger than 3 years. There were 3 of 7 cell lines (two ERMSs and one ARMS) and 2 of 17 fresh tumors (one ERMS and one ARMS) having less than a half of the mean DNA copy number, which suggested a loss of heterozygosity (LOH) in these samples; however, no homozygous deletion of *CDKN2A* was detected. The mRNA expression level of $p16^{INK4A}$ and $p14^{ARF}$ showed no obvious correlation with the relative DNA copy number.

Marked synergism between aberrant Met signaling and *Ink4a/Arf* inactivation has been shown to induce RMS at high frequency in mice (Sharp et al., 2002). Furthermore, *Pax3-Foxo1a* homozygosity with accompanying Ink4a/Arf or Tp53 pathway disruption substantially increases the frequency of alveolar RMS tumor formation in mice (Keller et al., 2004a). As shown in Figure 4A, 2 cell lines with overexpression of *MET* also had mutations of *TP53*; however, no cell lines with overexpression of *MET* showed reduced or absent expression of *CDKN2A*. Interestingly, all of the cell lines with reduced or absent expression of *CDKN2A* had mutations of *TP53*. Of 17 fresh tumors (Fig. 4B), 10 showed reduced or absent expression of *CDKN2A*; 2 of them with overexpression of *MET* and 1 of them having mutation of *TP53* simultaneously. One sample with overexpression of *MET* had mutation of *TP53*. Only 1 of 7 cell lines and 1 of 17 fresh tumors showed overexpression of *MET* alone, and one cell line and four fresh tumors did not show changes in any of the three genes.

In conclusion, our data suggest that *MET*, *CDKN2A* as well as *TP53* are involved in the pathogenesis of RMS, and that *MET* may play an important role in the progression of RMS. Molecules that specifically inhibit MET and HGF/SF are therefore promising in the treatment of RMS patients predicted to have poor prognosis.

ACKNOWLEDGMENTS

We thank Mrs. S. Soma, Miss E. Matsui, and Mrs. H. Soga for their excellent technical assistance.

REFERENCES

Birchmeier C, Birchmeier W, Gherardi E, Vande Woude GF. 2003. Met, metastasis, motility and more. Nat Rev Mol Cell Biol 4:915–925.

Bladt F, Riethmacher D, Isenmann S, Aguzzi A, Birchmeier C. 1995. Essential role for the c-met receptor in the migration of myogenic precursor cells into the limb bud. Nature 376:768–771.

Buckingham M, Bajard L, Chang T, Daubas P, Hadchouel J, Meilhac S, Montarras D, Rocancourt D, Relaix F. 2003. The formation of skeletal muscle: From somite to limb. J Anat 202:59–68.

Chen Y, Takita J, Hiwatari M, Igarashi T, Hanada R, Kikuchi A, Hongo T, Taki T, Ogasawara M, Shimada A, Hayashi Y. 2006. Mutations of the PTPN11 and RAS genes in rhabdomyosarcoma and pediatric hematological malignancies. Genes Chromosomes Cancer 45:583–591.

Chen YY, Takita J, Chen YZ, Yang HW, Hanada R, Yamamoto K, Hayashi Y. 2003. Genomic structure and mutational analysis of the human KIF1Bα gene located at 1p36.2 in neuroblastoma. Int J Oncol 23:737–744.

Chen YY, Takita J, Tanaka K, Ida K, Koh K, Igarashi T, Hanada R, Kikuchi A, Tanaka Y, Toyoda Y, Hayashi Y. 2005. Aberrations of the CHK2 gene are rare in pediatric solid tumors. Int J Mol Med 16:85–91.

Crist WM, Garnsey L, Beltangady MS, Gehan E, Ruymann F, Webber B, Hays DM, Wharam M, Maurer HM, Intergroup Rhabdomyosarcoma Committee. 1990. Prognosis in children with rhabdomyosarcoma: A report of the intergroup rhabdomyosarcoma studies I and II. J Clin Oncol 8:443–452.

Dagher R, Helman L. 1999. Rhabdomyosarcoma: An overview. Oncologist 4:34–44.

Dalle JH, Fournier M, Nelken B, Mazingue F, Lai JL, Bauters F, Fenaux P, Quesnel B. 2002. p16(INK4a) immunocytochemical analysis is an independent prognostic factor in childhood acute lymphoblastic leukemia. Blood 99:2620–2623.

Davis RJ, D'Cruz CM, Lovell MA, Biegel JA, Barr FG. 1994. Fusion of PAX7 to FKHR by the variant t(1;13)(p36;q14) translocation in alveolar rhabdomyosarcoma. Cancer Res 54:2869–2872.

Di Renzo MF, Olivero M, Ferro S, Prat M, Bongarzone I, Pilotti S, Belfiore A, Costantino A, Vigneri R, Pierotti MA, Comoglio PM. 1992. Overexpression of the c-MET/HGF receptor gene in human thyroid carcinomas. Oncogene 7:2549–2553.

Di Renzo MF, Poulsom R, Olivero M, Comoglio PM, Lemoine NR. 1995. Expression of the Met/hepatocyte growth factor receptor in human pancreatic cancer. Cancer Res 55:1129–1138.

Epstein JA, Shapiro DN, Cheng J, Lam PY, Maas RL. 1996. Pax3 modulates expression of the c-Met receptor during limb muscle development. Proc Natl Acad Sci USA 93:4213–4218.

Ferracini R, Di Renzo MF, Scotlandi K, Baldini N, Olivero M, Lollini P, Cremona O, Campanacci M, Comoglio PM. 1995. The Met/HGF receptor is over-expressed in human osteosarcomas and is activated by either a paracrine or an autocrine circuit. Oncogene 10:739–749.

Ferracini R, Olivero M, Di Renzo MF, Martano M, De Giovanni C, Nanni P, Basso G, Scotlandi K, Lollini PL, Comoglio PM. 1996. Retrogenic expression of the MET proto-oncogene correlates with the invasive phenotype of human rhabdomyosarcomas. Oncogene 12:1697–1705.

Galili N, Davis RJ, Fredericks WJ, Mukhopadhyay S, Rauscher FJ, III, Emanuel BS, Rovera G, Barr FG. 1993. Fusion of a fork head domain gene to PAX3 in the solid tumour alveolar rhabdomyosarcoma. Nat Genet 5:230–235.

Ginsberg JP, Davis RJ, Bennicelli JL, Nauta LE, Barr FG. 1998. Up-regulation of MET but not neural cell adhesion molecule expression by the PAX3-FKHR fusion protein in alveolar rhabdomyosarcoma. Cancer Res 58:3542–3546.

Giordano S, Di Renzo MF, Narsimhan RP, Cooper CS, Rosa C, Comoglio PM. 1989. Biosynthesis of the protein encoded by the c-met proto-oncogene. Oncogene 4:1383–1388.

Iolascon A, Faienza MF, Coppola B, Rosolen A, Basso G, Della Ragione F, Schettini F. 1996. Analysis of cyclin-dependent kinase inhibitor genes (CDKN2A, CDKN2B, and CDKN2C) in childhood rhabdomyosarcoma. Genes Chromosomes Cancer 15:217–222.

Jeffers M, Rong S, Woude GF. 1996. Hepatocyte growth factor/scatter factor-Met signaling in tumorigenicity and invasion/metastasis. J Mol Med 74:505–513.

Kamb A, Gruis NA, Weaver-Feldhaus J, Liu Q, Harshman K, Tavtigian SV, Stockert E, Day RS, III, Johnson BE, Skolnick MH. 1994. A cell cycle regulator potentially involved in genesis of many tumor types. Science 264:436–440.

Keller C, Arenkiel BR, Coffin CM, El-Bardeesy N, DePinho RA, Capecchi MR. 2004a. Alveolar rhabdomyosarcomas in conditional

Pax3: Fkhr mice: Cooperativity of Ink4a/ARF and Trp53 loss of function. Genes Dev 18:2614–2626.
Keller C, Hansen MS, Coffin CM, Capecchi MR. 2004b. Pax3: Fkhr interferes with embryonic Pax3 and Pax7 function: Implications for alveolar rhabdomyosarcoma cell of origin. Genes Dev 18: 2608–2613.
Lagutina I, Conway SJ, Sublett J, Grosveld GC. 2002. Pax3-FKHR knock-in mice show developmental aberrations but do not develop tumors. Mol Cell Biol 22:7204–7216.
Lillington DM, Goff LK, Kingston JE, Onadim Z, Price E, Domizio P, Young BD. 2002. High level amplification of N-MYC is not associated with adverse histology or outcome in primary retinoblastoma tumours. Br J Cancer 87:779–782.
Lorenzato A, Olivero M, Patane S, Rosso E, Oliaro A, Comoglio PM, Di Renzo MF. 2002. Novel somatic mutations of the MET oncogene in human carcinoma metastases activating cell motility and invasion. Cancer Res 62:7025–7030.
Matsumoto K, Nakamura T. 1996. Emerging multipotent aspects of hepatocyte growth factor. J Biochem (Tokyo) 119:591–600.
Mekki Y, Catallo R, Bertrand Y, Manel AM, Ffrench P, Baghdassarian N, Duhaut P, Bryon PA, Ffrench M. 1999. Enhanced expression of p16ink4a is associated with a poor prognosis in childhood acute lymphoblastic leukemia. Leukemia 13:181–189.
Merlino G, Helman LJ. 1999. Rhabdomyosarcoma—working out the pathways. Oncogene 18:5340–5348.
Newton WA, Jr., Gehan EA, Webber BL, Marsden HB, van Unnik AJ, Hamoudi AB, Tsokos MG, Shimada H, Harms D, Schmidt D, Ninfo V, Cavazzana AO, Gonzalez-Crussi F, Parham DM, Reiman HM, Asmar L, Beltangady MS, Sachs NE, Triche TJ, Maurer HM. 1995. Classification of rhabdomyosarcomas and related sarcomas. Pathologic aspects and proposal for a new classification—An Intergroup Rhabdomyosarcoma study. Cancer 76:1073–1085.
Ohnishi H, Kawamura M, Ida K, Sheng XM, Hanada R, Nobori T, Yamamori S, Hayashi Y. 1995. Homozygous deletions of p16/MTS1 gene are frequent but mutations are infrequent in childhood T-cell acute lymphoblastic leukemia. Blood 86:1269–1275.
Okamoto A, Demetrick DJ, Spillare EA, Hagiwara K, Hussain SP, Bennett WP, Forrester K, Gerwin B, Serrano M, Beach DH, Harris CC. 1994. Mutations and altered expression of p16INK4 in human cancer. Proc Natl Acad Sci USA 91:11045–11049.
Omura-Minamisawa M, Diccianni MB, Chang RC, Batova A, Bridgeman LJ, Schiff J, Cohn SL, London WB, Yu AL. 2001. p16/p14(ARF) cell cycle regulatory pathways in primary neuroblastoma: p16 expression is associated with advanced stage disease. Clin Cancer Res 7:3481–3490.
Orlow I, Roy P, Barz A, Canchola R, Song Y, Berwick M. 2001. Validation of denaturing high performance liquid chromatography as a rapid detection method for the identification of human INK4A gene mutations. J Mol Diagn 3:158–163.
Park WS, Dong SM, Kim SY, Na EY, Shin MS, Pi JH, Kim BJ, Bae JH, Hong YK, Lee KS, Lee SH, Yoo NJ, Jang JJ, Pack S, Zhuang Z, Schmidt L, Zbar B, Lee JY. 1999. Somatic mutations in the kinase domain of the Met/hepatocyte growth factor receptor gene in childhood hepatocellular carcinomas. Cancer Res 59:307–310.
Robertson KD, Jones PA. 1999. Tissue-specific alternative splicing in the human INK4a/ARF cell cycle regulatory locus. Oncogene 18:3810–3820.
Schmidt C, Bladt F, Goedecke S, Brinkmann V, Zschiesche W, Sharpe M, Gherardi E, Birchmeier C. 1995. Scatter factor/hepatocyte growth factor is essential for liver development. Nature 373:699–702.
Schmidt L, Duh FM, Chen F, Kishida T, Glenn G, Choyke P, Scherer SW, Zhuang Z, Lubensky I, Dean M, Allikmets R, Chidambaram A, Bergerheim UR, Feltis JT, Casadevall C, Zamarron A, Bernues M, Richard S, Lips CJ, Walther MM, Tsui LC, Geil L, Orcutt ML, Stackhouse T, Lipan J, Slife L, Brauch H, Decker J, Niehans G, Hughson MD, Moch H, Storkel S, Lerman MI, Linehan WM, Zbar B. 1997. Germline and somatic mutations in the tyrosine kinase domain of the MET proto-oncogene in papillary renal carcinomas. Nat Genet 16:68–73.
Sharp R, Recio JA, Jhappan C, Otsuka T, Liu S, Yu Y, Liu W, Anver M, Navid F, Helman LJ, DePinho RA, Merlino G. 2002. Synergism between INK4a/ARF inactivation and aberrant HGF/SF signaling in rhabdomyosarcomagenesis. Nat Med 8:1276–1280.
Sherr CJ. 2001. The INK4a/ARF network in tumour suppression. Nat Rev Mol Cell Biol 2:731–737.
Shibuya N, Taki T, Mugishima H, Chin M, Tsuchida M, Sako M, Kawa K, Ishii E, Miura I, Yanagisawa M, Hayashi Y. 2001. t(10;11)-acute leukemias with MLL-AF10 and MLL-ABI1 chimeric transcripts: Specific expression patterns of ABI1 gene in leukemia and solid tumor cell lines. Genes Chromosomes Cancer 32:1–10.
Skapek SX, Rhee J, Spicer DB, Lassar AB. 1995. Inhibition of myogenic differentiation in proliferating myoblasts by cyclin D1-dependent kinase. Science 267:1022–1024.
Sonnenberg E, Meyer D, Weidner KM, Birchmeier C. 1993. Scatter factor/hepatocyte growth factor and its receptor, the c-met tyrosine kinase, can mediate a signal exchange between mesenchyme and epithelia during mouse development. J Cell Biol 123:223–235.
Sorensen PH, Lynch JC, Qualman SJ, Tirabosco R, Lim JF, Maurer HM, Bridge JA, Crist WM, Triche TJ, Barr FG. 2002. PAX3-FKHR and PAX7-FKHR gene fusions are prognostic indicators in alveolar rhabdomyosarcoma: A report from the children's oncology group. J Clin Oncol 20:2672–2679.
Takeo S, Arai H, Kusano N, Harada T, Furuya T, Kawauchi S, Oga A, Hirano T, Yoshida T, Okita K, Sasaki K. 2001. Examination of oncogene amplification by genomic DNA microarray in hepatocellular carcinomas: Comparison with comparative genomic hybridization analysis. Cancer Genet Cytogenet 130:127–132.
Takita J, Hayashi Y, Kohno T, Yamaguchi N, Hanada R, Yamamoto K, Yokota J. 1997. Deletion map of chromosome 9 and p16 (CDKN2A) gene alterations in neuroblastoma. Cancer Res 57:907–912.
Takita J, Hayashi Y, Nakajima T, Adachi J, Tanaka T, Yamaguchi N, Ogawa Y, Hanada R, Yamamoto K, Yokota J. 1998. The p16 (CDKN2A) gene is involved in the growth of neuroblastoma cells and its expression is associated with prognosis of neuroblastoma patients. Oncogene 17:3137–3143.
Takita J, Ishii M, Tsutsumi S, Tanaka Y, Kato K, Toyoda Y, Hanada R, Yamamoto K, Hayashi Y, Aburatani H. 2004. Gene expression profiling and identification of novel prognostic marker genes in neuroblastoma. Genes Chromosomes Cancer 40:120–132.
Taulli R, Scuoppo C, Bersani F, Accornero P, Forni PE, Miretti S, Grinza A, Allegra P, Schmitt-Ney M, Crepaldi T, Ponzetto C. 2006. Validation of met as a therapeutic target in alveolar and embryonal rhabdomyosarcoma. Cancer Res 66:4742–4749.
Trusolino L, Comoglio PM. 2002. Scatter-factor and semaphorin receptors: Cell signalling for invasive growth. Nat Rev Cancer 2:289–300.
Tuck AB, Park M, Sterns EE, Boag A, Elliott BE. 1996. Coexpression of hepatocyte growth factor and receptor (Met) in human breast carcinoma. Am J Pathol 148:225–232.
Uehara Y, Minowa O, Mori C, Shiota K, Kuno J, Noda T, Kitamura N. 1995. Placental defect and embryonic lethality in mice lacking hepatocyte growth factor/scatter factor. Nature 373:702–705.
Uno K, Takita J, Yokomori K, Tanaka Y, Ohta S, Shimada H, Gilles FH, Sugita K, Abe S, Sako M, Hashizume K, Hayashi Y. 2002. Aberrations of the hSNF5/INI1 gene are restricted to malignant rhabdoid tumors or atypical teratoid/rhabdoid tumors in pediatric solid tumors. Genes Chromosomes Cancer 34:33–41.
Zhang Y, Xiong Y, Yarbrough WG. 1998. ARF promotes MDM2 degradation and stabilizes p53: ARF-INK4a locus deletion impairs both the Rb and p53 tumor suppression pathways. Cell 92:725–734.

International Journal of
HEMATOLOGY

Letter to the Editor

Low Frequency of *KIT* Gene Mutation in Pediatric Acute Myeloid Leukemia with inv(16)(p13q22): A Study of the Japanese Childhood AML Cooperative Study Group

Akira Shimada,[a] Hitoshi Ichikawa,[b] Tomohiko Taki,[c] Chisato Kubota,[a] Teruaki Hongo,[d] Masahiro Sako,[e] Akira Morimoto,[f] Akio Tawa,[g] Ichiro Tsukimoto,[h] Yasuhide Hayashi[a]

[a]Department of Hematology/Oncology, Gunma Children's Medical Center, Gunma, Japan; [b]Cancer Transcriptome Project, National Cancer Center Research Institute, Tokyo, Japan; [c]Department of Molecular Laboratory Medicine, Kyoto Prefectural University of Medicine Graduate School of Medical Science, Kyoto, Japan; [d]Department of Pediatrics, Hamamatsu University School of Medicine, Shizuoka, Japan; [e]Department of Pediatric Hematology/Oncology, Osaka City General Hospital, Osaka, Japan; [f]Department of Pediatrics, Kyoto Prefectural University of Medicine Graduate School of Medical Science, Kyoto, Japan; [g]Department of Pediatrics, National Hospital Organization Osaka National Hospital, Osaka, Japan; [h]First Department of Pediatrics, Toho University School of Medicine, Tokyo, Japan

Received June 6, 2007; received in revised form June 21, 2007; accepted June 28, 2007

Int J Hematol. 2007;86:289-290. doi: 10.1532/IJH97.07098

Acute myeloid leukemia (AML) patients with t(8;21)(q22;q22) or inv(16)(p13q22) are known to have a good prognosis. Recently, mutations of the *KIT* gene have been found in 12.7% to 48.1% of adult AML patients with t(8;21) or inv(16) and in approximately 20% of pediatric AML patients with t(8;21) [1-5]. *KIT* gene mutations in adult and pediatric AML patients with t(8;21) and in adult AML patients with inv(16) have been associated with a poorer prognosis than in those without *KIT* gene mutations [1-5]. However, the frequency and clinical impact of *KIT* gene mutations in pediatric AML patients with inv(16) remain unknown. Pediatric AML patients with inv(16) have been reported to represent 3.4% to 6% of the total number of pediatric AML patients. Thus, the number of patients in this subgroup is very small [6,7].

Three hundred eighteen patients were enrolled in the Japanese Childhood AML Cooperative Study Group Protocol AML 99 from January 2000 to December 2002, and 12 (3.8%) of these AML patients comprised 11 patients with inv(16) and 1 patient with t(16;16)(p13;q22) [5,8]. The 5-year overall survival rate was 100%, and the event-free survival rate was 90.9%. Of these 12 AML patients with inv(16) or t(16;16), 7 patients were available for molecular analysis (age range, 11 months to 14 years; median, 10 years) (Table 1). The 5-year overall survival rate for these 7 patients was 100%, and the event-free survival rate was 85.7% (Table 1). We used the reverse transcriptase–polymerase chain reaction method in a mutational analysis of the extracellular domain (exons 8 and 9), the transmembrane domain (exon 10), the juxtamembrane domain (exon 11), and the second intracellular kinase domain (exons 17 and 18) of the *KIT* gene and then carried out a sequencing analysis [5]. Sequencing was performed directly or, if necessary, after subcloning.

KIT mutation (deletion of D419 in exon 8) was found in an 11-month-old male patient (1 [14.3%] of 7 patients). The initial white blood cell count for this patient (no. 7) was 199,000/μL, and a karyotype analysis revealed 46,XY,inv(16)(p13q22). This patient received a total of 6 consecutive chemotherapies; however, he relapsed 16 months after the initial diagnosis. He then underwent unrelated allogeneic stem cell transplantation during the second complete remission and has been alive for 40 months from the diagnosis. The remaining 6 AML patients with inv(16) have maintained a complete remission without relapse for more than 41 months.

As for *FLT3* and *RAS* gene alterations, we found 2 *FLT3* D835 mutations (28.6%) and 2 *NRAS* mutations (28.6%) in these 7 AML patients with inv(16) (Table 1). No patient had an *FLT3* internal tandem duplication or a *KRAS* gene mutation. The majority of these patients (5 [71.4%] of 7) had one of the chimeric *CBFβ-MYH11* transcripts, which have most frequently been found in AML cases with inv(16) (*CBFβ* at nucleotide 495 fused to

Correspondence and reprint requests: Yasuhide Hayashi, MD, Director, Gunma Children's Medical Center, 779 Shimohakoda, Hokkitsu, Shibukawa, Gunma 377-8577, Japan; 81-279-52-3551 ext 201; fax: 81-279-52-2045 (e-mail: hayashiy-tky@umin.ac.jp).

Table 1.
Correlations of Clinical Features with *KIT*, *FLT3*, and *RAS* Gene Mutations in 7 Acute Myeloid Leukemia Patients with inv(16) or t(16;16)*

Patient No.	Age	Sex	FAB Classification	Karyotype	*CBFβ-MYH11*	*KIT* Mt	*FLT3* D835 Mt	*NRAS* Mt	EFS Time, mo
1	14 y	M	M4Eo	46,XY,inv(16)(p13q22), add(7)(q32)	†	–	–	+‡	63+
2	10 y	M	M4Eo	46,XY,inv(16)(p13q22)	1	–	–	–	67+
3	7 y	M	M1	46,XY,inv(16)(p13q22)	1	–	–	–	63+
4	13 y	F	M1	46,XX,inv(16)(p13q22)	1	–	+	–	59+
5	3 y	F	M5a	47,XX,+8,t(16;16)(p13;q22)	2	–	–	+‡	43+
6	14 y	F	M5b	46,XX,inv(16)(p13q22)	1	–	+	–	41+
7	11 mo	M	M4Eo	46,XY,inv(16)(p13q22)	1	+§	–	–	16

**CBFβ-MYH11* transcripts were detected by reverse transcriptase–polymerase chain reaction analysis and direct sequencing (1, nucleotide 495 of *CBFβ* fused to nucleotide 1921 of *MYH11*; 2, nucleotide 399 of *CBFβ* fused to nucleotide 1201 of *MYH11*). *KRAS* mutations were not found in any of the 7 patients. FAB, French-American-British; Mt, mutation; EFS, event-free survival.

†Chimeric transcripts were not detected.

‡Codon 12.

§Deletion D419 in exon 8.

MYH11 at nucleotide 1921, Table 1) [9,10]. The *FLT3* D835 mutation, *NRAS* mutation, and subtypes of *CBFβ-MYH11* transcripts were not associated with the clinical outcome.

We also looked for *KIT* mutations in 11 pediatric AML patients with inv(16) who were treated with the previous protocol in Japan (age range, 8 months to 15 years; median, 3 years), but we did not identify *KIT* mutations in any of the patients. Interestingly, 3 of the 11 AML patients with inv(16) were infants, and 2 of them died, although all 3 exhibited no mutations in *KIT*, *FLT3*, or *RAS*. These data together with those described in our previous report [11] suggest that infant AML patients with inv(16) have a poor prognosis, regardless of the status of these genes.

A few reports have suggested that adult AML patients who have inv(16) with *KIT* mutations were associated with a poorer prognosis than those without KIT mutations [2,3]. A recent study by the Berlin-Frankfurt-Münster Study Group revealed that 6 (54.5%) of 11 pediatric AML patients with inv(16) had *KIT* mutations but that the clinical impact was limited [12]. The Acute Leukemia French Association (ALFA) and the Leucémies Aiguës Myéloblastiques de l'Enfant (LAME) cooperative study groups also suggested that *KIT* gene mutations were not associated with a poor prognosis in pediatric and adult AML patients with inv(16) [4]. We considered the frequency of *KIT* gene mutations (1 [5.6%] of 18) among the pediatric AML patients with inv(16) in this study to be lower than that of adult AML patients with inv(16) [2-4]. We must await the results of a larger study regarding the correlation between *KIT* gene mutations and prognosis in pediatric AML patients with inv(16).

Acknowledgments

This work was supported in part by a Grant-in-Aid for Cancer Research and a Grant for Clinical Cancer Research and Research on Children and Families from the Ministry of Health, Labor and Welfare of Japan. This work was also supported by a Grant-in-Aid for Scientific Research (C) from the Ministry of Education, Culture, Sports, Science and Technology of Japan and a Research Grant for Gunma Prefectural Hospitals.

References

1. Beghini A, Peterlongo P, Ripamonti CB, et al. C-kit mutations in core binding factor leukemias. *Blood.* 2000;95:726-727.
2. Care RS, Valk PJ, Goodeve AC, et al. Incidence and prognosis of c-KIT and FLT3 mutations in core binding factor (CBF) acute myeloid leukaemias. *Br J Haematol.* 2003;121:775-777.
3. Paschka P, Marcucci G, Ruppert AS, et al. Adverse prognostic significance of KIT mutations in adult acute myeloid leukemia with inv(16) and t(8;21): a Cancer and Leukemia Group B study. *J Clin Oncol.* 2006;24:3904-3911.
4. Boissel N, Leroy H, Brethon B, et al, for the Acute Leukemia French Association (ALFA) and the Leucémies Aiguës Myéloblastiques de l'Enfant (LAME) Cooperative Groups. Incidence and prognostic impact of c-Kit, FLT3, and Ras gene mutations in core binding factor acute myeloid leukemia (CBF-AML). *Leukemia.* 2006;20:965-970.
5. Shimada A, Taki T, Tabuchi K, et al. KIT mutations, and not FLT3 internal tandem duplication, are strongly associated with a poor prognosis in pediatric acute myeloid leukemia with t(8;21): a study of the Japanese Childhood AML Cooperative Study Group. *Blood.* 2006;107:1806-1809.
6. Grimwade D, Walker H, Oliver F, et al, on behalf of the Medical Research Council Adult and Children's Leukaemia Working Parties. The importance of diagnostic cytogenetics on outcome in AML: analysis of 1,612 patients entered into the MRC AML 10 trial. *Blood.* 1998;92:2322-2333.
7. Forestier E, Heim S, Blennow E, et al. Cytogenetic abnormalities in childhood acute myeloid leukaemia: a Nordic series comprising all children enrolled in the NOPHO-93-AML trial between 1993 and 2001. *Br J Haematol.* 2003;121:566-577.
8. Kobayashi R, Tawa A, Hanada R, Horibe K, Tsuchida M, Tsukimoto I, for the Japanese childhood AML cooperative study group. Extramedullary infiltration at diagnosis and prognosis in children with acute myelogenous leukemia. *Pediatr Blood Cancer.* 2007;48:393-398.
9. Poirel H, Radford-Weiss I, Rack K, et al. Detection of the chromosome 16 CBF beta-MYH11 fusion transcript in myelomonocytic leukemias. *Blood.* 1995;85:1313-1322.
10. Reilly JT. Pathogenesis of acute myeloid leukaemia and inv(16)(p13;q22): a paradigm for understanding leukaemogenesis? *Br J Haematol.* 2005;128:18-34.
11. Xu F, Taki T, Eguchi M, et al. Tandem duplication of the FLT3 gene is infrequent in infant acute leukemia. Japan Infant Leukemia Study Group. *Leukemia.* 2000;14:945-947.
12. Goemans BF, Zwaan CM, Miller M, et al. Mutations in KIT and RAS are frequent events in pediatric core-binding factor acute myeloid leukemia. *Leukemia.* 2005;19:1536-1542.

Research Article

Fms-like Tyrosine Kinase 3 Ligand Stimulation Induces *MLL*-Rearranged Leukemia Cells into Quiescence Resistant to Antileukemic Agents

Yoshiyuki Furuichi,[1] Kumiko Goi,[1] Takeshi Inukai,[1] Hiroki Sato,[1] Atsushi Nemoto,[1] Kazuya Takahashi,[1] Koshi Akahane,[1] Kinuko Hirose,[1] Hiroko Honna,[1] Itaru Kuroda,[1] Xiaochun Zhang,[1] Keiko Kagami,[1] Yasuhide Hayashi,[2] Kenichi Harigaya,[3] Shinpei Nakazawa,[1] and Kanji Sugita[1]

[1]Department of Pediatrics, School of Medicine, University of Yamanashi, Yamanashi, Japan; [2]Department of Hematology and Oncology, Gunma Children's Medical Center, Gunma, Japan; and [3]Molecular and Tumor Pathology, Graduate School of Medicine, Chiba University, Chiba, Japan

Abstract

Fms-like tyrosine kinase 3 (FLT3) is highly expressed in acute lymphoblastic leukemia with the *mixed-lineage leukemia* (*MLL*) gene rearrangement refractory to chemotherapy. We examined the biological effect of FLT3-ligand (FL) on 18 B-precursor leukemic cell lines with variable karyotypic abnormalities, and found that nine of nine *MLL*-rearranged cell lines with wild-type FLT3, in contrast to other leukemic cell lines, are significantly inhibited in their proliferation in a dose-dependent manner by FL. This inhibition was due to induction of the G_0-G_1 arrest. A marked up-regulation of p27 by suppression of its protein degradation and an abrogation of constitutive signal transducers and activators of transcription 5 phosphorylation were revealed in arrested leukemia cells after FL stimulation. Importantly, FL treatment rendered not only cell lines but also primary leukemia cells with *MLL* rearrangement resistant to chemotherapeutic agents. *MLL*-rearranged leukemia cells adhering to the bone marrow stromal cell line, which expresses FL as the membrane-bound form, were induced to quiescent state resistant to chemotherapeutic agents, but their chemosensitivity was significantly restored in the presence of neutralizing anti-FL antibody. The FL/FLT3 interaction between leukemia cells and bone marrow stromal cells expressing FL at high levels should contribute, at least in part, to persistent minimal-residual disease of *MLL*-rearranged leukemia in bone marrow. [Cancer Res 2007;67(20):9852–61]

Introduction

Fms-like tyrosine kinase 3 (FLT3) belongs to the receptor tyrosine kinase class III family and plays an important role in an early stage of hematopoiesis (1–3). In normal bone marrow, FLT3 is expressed predominantly in hematopoietic stem/progenitor cells (2, 4) and FLT3-ligand (FL) shows a strong synergy with other cytokines in their proliferation (5, 6). FLT3 is also expressed at considerable levels in most clinical samples from acute myelogenous leukemia (AML) and B-precursor acute lymphoblastic leukemia (ALL) patients (7, 8). However, the growth-promoting activity of FL alone in AML and ALL cells is heterogeneous and rather modest in comparison with other effective cytokines (6, 8, 9). Recently, two types of FLT3 mutations were found in leukemic cells, which activate constitutively the FLT3 tyrosine kinase. One is internal tandem duplications (ITD) in the juxtamembrane domain of FLT3 (10), and the other is a point mutation of D835/I836 within the activation loop of the second tyrosine kinase domain of FLT3 (FLT3-TK mutation; refs. 11, 12). Although less frequently, active point mutations other than D835/I836 have been known in the juxtamembrane domain of FLT3. Several studies have shown that FLT3-ITDs confer a poor prognosis in adult AML (13, 14) and in childhood AML (15, 16).

The *mixed-lineage leukemia* (*MLL*) gene rearrangement results from chromosomal translocation at 11q23, and frequently observed in infantile ALL and therapy-related secondary leukemia with a very poor prognosis (17, 18). Armstrong et al. (19) reported that *MLL*-rearranged leukemia has a highly distinct gene expression profile that is consistent with the developmental stage of a very early hematopoietic progenitor, and that the *FLT3* gene is the most differentially expressed gene that distinguishes *MLL*-rearranged leukemia from other subtypes of ALL and AML. We recently showed that a FLT3-TK mutation is also detected in 16% of *MLL*-rearranged ALL in infants (20). Under the hypothesis that constitutive activation of FLT3 might be involved in maintenance and development of *MLL*-rearranged leukemia as a second hit, new therapeutic approaches using FLT3-targeted tyrosine kinase inhibitors are emerging for the treatment of *MLL*-rearranged leukemia overexpressing FLT3 with or without activating mutations (21, 22).

In the present study, we showed that FL stimulation specifically induced *MLL*-rearranged leukemia cells into quiescence resistant to antileukemic agents, and postulated that the FL/FLT3 interaction possibly implicated in the formation of minimal residual disease (MRD) of this leukemia.

Materials and Methods

Human cell lines and primary leukemia cells. Twenty human lymphoid leukemic cell lines were used in this study. Eighteen were B-lineage including 10 with *MLL* rearrangement, 4 with Philadelphia chromosome (Ph1), and 4 with other karyotypes. Two T-lineage cell lines were also used as controls. All cell lines have been established in our laboratory and are maintained in RPMI 1640 supplemented with 10% FCS as reported previously (23, 24). Their characteristics are summarized in

Note: Supplementary data for this article are available at Cancer Research Online (http://cancerres.aacrjournals.org/).

Requests for reprints: Kanji Sugita, Department of Pediatrics, School of Medicine, University of Yamanashi, 1110 Shimokato, Chuo, Yamanashi 409-3898, Japan. Phone: 81-55-273-9606; Fax: 81-55-273-6745; E-mail: ksugita@yamanashi.ac.jp.

doi:10.1158/0008-5472.CAN-07-0105

Table 1. Characteristics of B-precursor leukemic cell lines and their FLT3 expression

	Surface antigens			Karyotype	FLT3 expression	
	CD 10	19	13		%	MFI
MLL rearrangement						
KOCL-33	−	+	−	t(11;19)(q23;p13)	99	204.1
KOCL-44	−	+	−	t(11;19)(q23;p13)	99	340.1
KOCL-45	−	+	+	t(4;11)(q21;q23)	95	115.0
KOCL-50	−	+	−	t(11;19)(q23;p13)	77	80.3
KOCL-51	−	+	+	t(11;19)(q23;p13)	98	162.1
KOCL-58	−	+	+	t(4;11)(q21;q23)	79	41.9
KOCL-69	−	+	+	t(4;11)(q21;q23)	57	63.6
KOPN-1	−	+	−	t(11;19)(q23;p13)	94	169.1
KOPB-26	−	+	−	t(9;11)(p22;q23)	99	1046.8
YACL-95	+	+	−	t(9;11)(p22;q23)	98	381.3
MLL germ line						
KOPN-30bi	+	+	+	t(9;22)(q34;p11.2)*	88	75.1
KOPN-55bi	+	+	+	t(9;22)(q34;p11.2)†	90	367.0
KOPN-57bi	+	+	+	t(9;22)(q34;p11.2)*	99	581.7
KOPN-72bi	+	+	+	t(9;22)(q34;p11.2)*	99	266.3
KOPN-32	−	+	−	t(5;11)(q31;q21)	73	54.0
KOPN-36	+	+	−	t(1;19)(q23;p13.3)	22	53.3
YAMN-92	+	+	−	t(1;19)(q23;p13.3)	28	43.8
KOPN-70	+	+	−	-X,-4,-17,+3mar	98	329.5

Abbreviation: MFI, mean fluorescence intensity.
*Minor bcr-abl.
† Major bcr-abl.

Table 1. KOCL-33 with t(11;19) is a special cell line with a D835 point mutation of FLT3 (20), whereas other cell lines with or without *MLL* gene rearrangement had neither FLT3-TK mutation nor ITDs. Human bone marrow stromal cell line KM-104 was used as the feeder expressing FL as the membrane-bound form (25). Fourteen primary leukemia samples with (n = 9) and without (n = 5) *MLL* rearrangement were also used after obtaining written informed consents.

Antibodies and reagents. FL was purchased from Peprotech. Biotinylated FL and neutralizing anti-FL monoclonal antibody (mAb) were purchased from R&D Systems. Cycloheximide, bromodeoxyuridine (BrdUrd), and propidium iodide were purchased from Sigma. Daunorubicin and 1-β-D-arabinofuranosylcytosine (AraC) were obtained from Meiji Seika and Nippon Shinyaku, respectively. PKC412 (*N*-benzoylstaurosporine, a FLT3 kinase inhibitor) was kindly provided by Novartis. Polyclonal antibodies against phosphorylated signal transducers and activators of transcription 5 (STAT5; Tyr^{694}), p44/42 mitogen-activated protein kinase (MAPK), phosphorylated p44/42MAPK (Thr^{202}/Tyr^{204}), Akt, and phosphorylated Akt (Ser^{473}) were purchased from Cell Signaling Technology; polyclonal antibodies against cyclin-dependent kinase 4 (CDK4), cyclin E, and p27 were from Upstate Biotechnology, Inc.; CDK2 was from PharMingen; and cyclin A was from Santa Cruz Biotechnology. mAbs against cyclin B, cyclin D3, and STAT5 were purchased from Transduction Laboratories; phosphotyrosine, CDK6, p21, c-Myc, and α-tubulin were from UBI, Lab Vision Corporation, PharMingen, Santa Cruz Biotechnology, and Sanbio, respectively.

Flow cytometric analysis. For FLT3 expression, 5×10^5 leukemia cells were incubated with biotinylated FL for 1 h at 4°C followed by incubation with avidin-FITC for 30 min at 4°C. As a negative staining control, anti-FL blocking antibody was mixed with FL-biotin. For FL expression, cells were incubated with biotinylated anti-FL antibody followed by incubation with avidin-FITC. IgG-biotin was used for a negative staining control. These cells were washed and analyzed using a flow cytometer (FACSCalibur, Becton Dickinson).

[^{3}H]thymidine uptake analysis. Leukemia cells (2.5×10^4 to 5×10^4 per well) were cultured in RPMI 1640 supplemented with 10% FCS in a 96-well flat-bottomed culture plate in triplicate in the presence or absence of various concentrations of FL at 37°C for the indicated periods. Subsequently, wells were pulsed with [^{3}H]thymidine (1 μCi/well) for 4 h, after which the cells were harvested onto glass-fiber filters. In some experiments, a FLT3 kinase inhibitor, PKC412, was included at various concentrations. [^{3}H]thymidine incorporated to DNA was measured using a liquid scintillation counter. Percentage stimulation was calculated as follows: {[(cpm of treated) / (cpm of untreated)] − 1} × 100. Percentage thymidine uptake was calculated as follows: {(cpm of treated) / (cpm of untreated)} × 100.

Cell cycle analysis. Leukemia cells (5×10^5/mL) were cultured in the presence or absence of FL (20 ng/mL) for 3 days. These cells were pulsed with BrdUrd for 30 min at 37°C and harvested. After fixation in 70% ethanol on ice, cells were treated with RNase (Funakoshi) for 15 min at 37°C, and subsequently washed with 4 N HCl, 0.1 mol/L $Na_2B_4O_7$, and 0.5% Tween 20. Cells were stained with FITC-conjugated anti-BrdUrd antibody for 20 min at 37°C and then treated with propidium iodide (50 μg/mL) for 20 min on ice. The signals generated by FITC and propidium iodide were analyzed using a flow cytometer.

Apoptosis analysis. Leukemia cells (5×10^5/mL) were incubated for 24 h in the presence or absence of FL (20 ng/mL) and then irradiated (4 Gy) followed by culture for 48 h, or exposed to daunorubicin (10 ng/mL) or AraC (200 nmol/L) for 48 h. Cells were then harvested and stained doubly with FITC-conjugated Annexin V and propidium iodide (MEBCYTO Apoptosis Detection Kit; MBL) at 37°C for 15 min in dark. Ten thousand events were analyzed using a flow cytometer.

Western blot analysis. Leukemia cells were solubilized in lysis buffer [50 mmol/L Tris-HCl (pH 7.5), containing 150 mmol/L NaCl, 1% NP40, 5 mmol/L EDTA, 0.05% NaN_3, 0.2 TIU/mL aprotinin, 1 μg/mL pepstatin A, 10 mmol/L iodoacetamide, 1 mmol/L phenylmethylsulfonyl fluoride, and 1 mmol/L sodium vanadate]. SDS was added to the lysis buffer

at a final concentration of 0.1% for analysis of nuclear proteins. The lysates were separated on a 6% to 15% SDS-polyacrylamide gel under reducing conditions and transferred to nitrocellulose membranes, which were incubated with various primary antibodies at 4°C overnight, and then with horseradish peroxidase–conjugated second antibody for 1 h at room temperature. The detection of the bands was done using an enhanced chemiluminescence kit (Amersham Japan).

RNase protection assays. Leukemia cells (5×10^5/mL) were cultured in the presence or absence of FL (20 ng/mL) for 24, 48, and 72 h, and their total RNAs were extracted. The RNase protection assay was done using [^{32}P]UTP-labeled multiprobe template hCC-1 and the RiboQuant Multi-Probe RNase Protection Assay system (PharMingen).

Dye-exclusion test. Leukemic cell lines (4×10^4/well) were precultured in the presence or absence of FL (20 ng/mL) for 24 h, and then exposed to daunorubicin (10–20 ng/mL) or AraC (200–400 nmol/L) for the indicated hours. In some experiments, the human bone marrow–derived stromal cell line KM-104 was used as the feeder. In analysis of primary samples, leukemia cells (1×10^5/well) were precultured in the presence or absence of FL (40 ng/mL) or KM-104 cells with or without anti-FL antibody for 24 h, and then exposed to AraC (100 nmol/L) for 24 h. The numbers of living and dead cells were counted by dye-exclusion test in triplicate after each of culture conditions, and viability (%) and Δviability (treated viability − control viability) were calculated.

Statistics. The Mann-Whitney's test was used for the comparison of the differences in FLT3 expression among leukemic cell lines and fresh leukemia cells, and unpaired *t* test for the comparison of the differences in [^{3}H]thymidine uptake and dye-exclusion analyses. Differences in the Δviabilities of primary leukemia cells between culture conditions were analyzed using the matched paired Wilcoxon's test. A P value of <0.05 was considered significant.

Results

Surface expression of FLT3 in leukemic cell lines. Surface expression of FLT3 in leukemic cell lines used in this study was first checked. B-precursor cell lines (n = 18) expressed a considerable amount of FLT3 on their surfaces (median 94.5%, range 22–99%) as shown in Table 1, whereas T-lineage cell lines (n = 2) did not (<10%; data not shown). There were no significant differences in percentage of FLT3-positive cells between B-precursor cell lines with (n = 10) and without (n = 8) *MLL* rearrangement (median of positive population; 96.5% versus 89.0%). There were also no significant differences in the FLT3 expression levels between B-precursor cell lines with and without *MLL* rearrangement (median of mean fluorescence intensity; 165.6 versus 170.7).

FL stimulation inhibits proliferation of *MLL*-rearranged leukemia cells by induction of cell cycle arrest. To investigate the biological effect of FL, 18 B-precursor leukemic cell lines were incubated in the presence or absence of various concentrations of FL for 72 h, and their [^{3}H]thymidine uptakes were assayed in the final 4-h incubation. As shown in Fig. 1*A*, three of four Ph1-positive leukemic cell lines showed stimulative responses to FL in a dose-dependent manner. Two of other four B-precursor cell lines without *MLL* rearrangement also showed a marked stimulative response to FL. Unexpectedly, however, all of the *MLL*-rearranged cell lines with wild-type FLT3 (n = 9), irrespective of the types of translocation, showed inhibitory responses to FL in a dose-dependent manner as shown in Fig. 1*B*. The *MLL*-rearranged cell line with a D835 mutation, KOCL-33, was not affected by the addition of FL. The kinetics of [^{3}H]thymidine uptakes after FL stimulation (20 ng/mL) was next analyzed using representative cell lines. The FL-induced inhibition in *MLL*-rearranged KOCL-51 and KOCL-58 reached maximal levels between 48 and 96 h of culture, whereas the FL-induced stimulation in KOPN-55bi (Ph1), KOPN-36 with t(1;19), and KOPN-70 (other B-precursor) peaked between 96 and 144 h of culture (data not shown). These results indicate that,

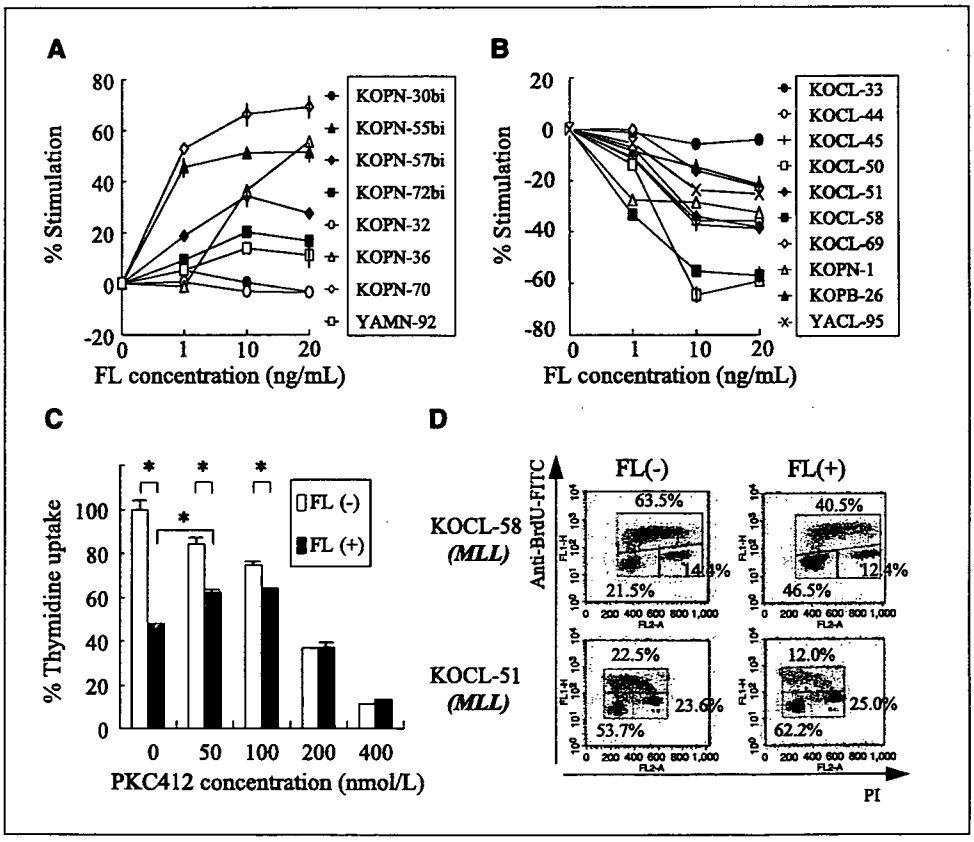

Figure 1. Effect of FL on [^{3}H]thymidine uptakes and cell cycle progression in B-precursor leukemic cell lines. In [^{3}H]thymidine uptake analysis, leukemic cell lines were cultured in triplicate in the presence or absence of FL for 72 h, pulsed, and harvested. Data are representative of three separate experiments and are shown as the mean. In cell cycle analysis, *MLL*-rearranged KOCL-58 and KOCL-51 cells were cultured in the presence or absence of FL (20 ng/mL) for 72 h, and stained with FITC-conjugated BrdUrd and propidium iodide. *A*, % stimulation of [^{3}H]thymidine uptakes by various concentrations of FL in Ph1-positive (n = 4, *closed symbols*) and other B-precursor cell lines without *MLL* rearrangement (n = 4, *open symbols*). *Bars*, SE >3%. *B*, % stimulation of [^{3}H]thymidine uptakes by various concentrations of FL in *MLL*-rearranged leukemic cell lines (n = 10). KOCL-33 is a special cell line with a D835 mutation of FLT3. *Bars*, SE >3%. *C*, effect of the FLT3 inhibitor (PKC412) on % thymidine uptake. *MLL*-rearranged KOCL-58 cells were cultured in the presence or absence of FL (20 ng/mL) with or without the addition of various concentrations of PKC412 (50–400 nmol/L), and % thymidine uptake was determined in each of culture conditions. *, P < 0.01, significant difference by t test. *D*, flow cytometric analysis of cell cycle progression. *Vertical* and *horizontal axes*, log fluorescence intensities of FITC and propidium iodide (*PI*), respectively.

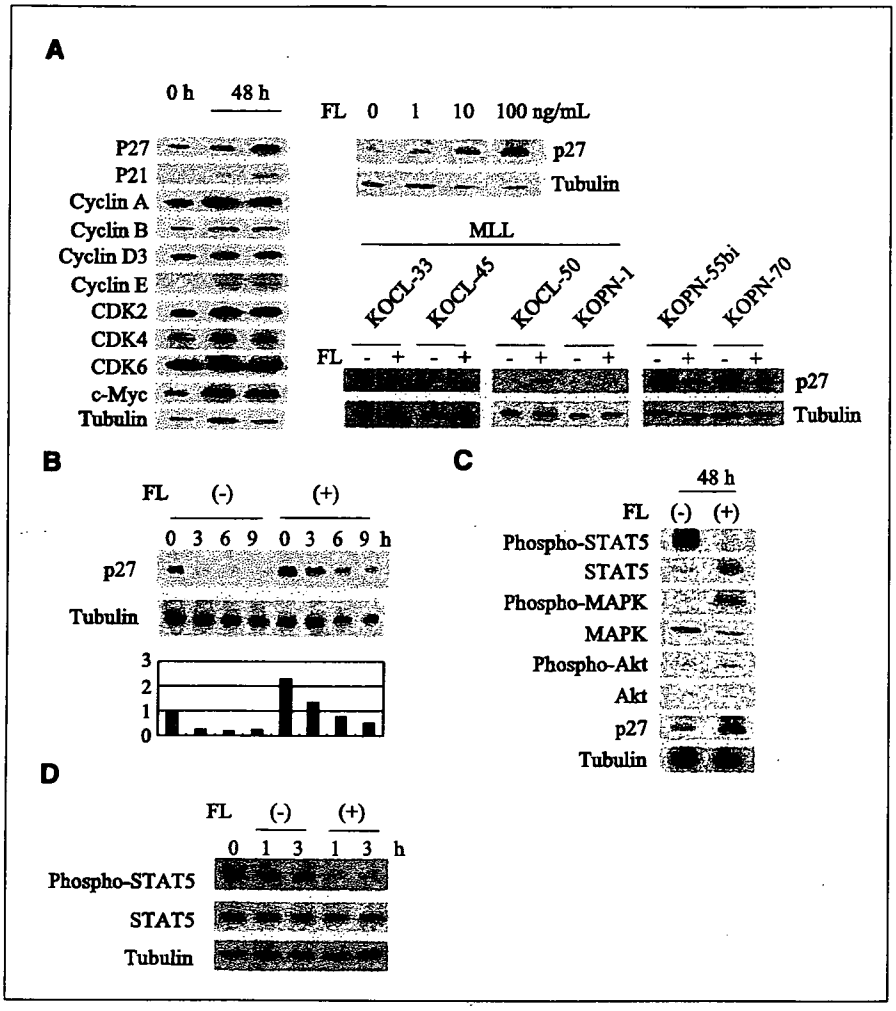

Figure 2. Changes in expression of cell cycle–related proteins and phosphorylation of FLT3-mediating signal transducing molecules after FL stimulation in *MLL*-rearranged leukemia cells. *A*, Western blot analysis of changes in expression of cell cycle–related proteins at 48 h after culture in the presence or absence of FL (20 ng/mL). *Left*, changes in expression of p27, p21; cyclins A, B, D3, and E; CDK2, CDK4, and CDK6; and c-Myc were examined in KOCL-58 cells. *Right, top*, changes in expression of p27 were examined in KOCL-58 cells after culture with increasing concentrations of FL; *bottom*, changes in expression of p27 were examined in leukemic cell lines with ($n = 4$) or without ($n = 2$) *MLL* rearrangement. *B*, half-life of p27 after FL stimulation. KOCL-58 cells were incubated for 24 h in the presence or absence of FL (20 ng/mL), further incubated in the presence of cycloheximide, and harvested at indicated time points. Changes in the p27 expression were measured by densitometry and half-life of p27 was calculated. Data are representative of three separate experiments. *C*, Western blot analysis of changes in phosphorylation of STAT5, MAPK, and Akt after FL stimulation. KOCL-58 cells were incubated for 48 h in the presence or absence of FL (20 ng/mL). *D*, Western blot analysis of changes in STAT5 phosphorylation after FL stimulation. KOCL-58 cells were incubated for 1 or 3 h in the presence or absence of FL (20 ng/mL).

in contrast to other types of leukemia cells, proliferation of *MLL*-rearranged leukemia cells with wild-type FLT3 is specifically suppressed by ligand activation of FLT3.

To determine whether the inhibitory effect of FL is dependent on the kinase activity of FLT3, *MLL*-rearranged KOCL-58 cells were cultured with or without FL (20 ng/mL) for 72 h in the presence of various concentrations of the FLT3 kinase inhibitor PKC412. As shown in Fig. 1*C*, PKC412 alone inhibited [^{3}H]thymidine uptake of KOCL-58 cells, as previously reported (21). Of note, thymidine uptake, which was inhibited by FL to 47.8% of the control level, was restored to 62.3% in the presence of 50 nmol/L PKC412, a concentration that can markedly suppress FLT3-mediating signal transduction molecules such as STAT5, MAPK, and Akt (Supplementary Fig. S1). This result suggests that the kinase activity of FLT3 is required for the FL-induced growth inhibition exhibited by *MLL*-rearranged leukemia cells.

To investigate the mechanism of the FL-induced growth inhibition seen in *MLL*-rearranged cell lines, cell cycle analysis was done at 72 h after FL treatment (20 ng/mL) using the BrdUrd/propidium iodide double staining method (Fig. 1*D*). In both KOCL-58 and KOCL-51 cell lines, the population in S phase after FL stimulation significantly decreased compared with that measured without FL stimulation with a concomitant increase in the population in G_0-G_1 phase. The population of cells in G_2-M phase remained unchanged after FL stimulation. Importantly, the apoptotic population, which appears in the hypodiploid region, did not increase in either cell line. These results were consistently observed in three separate experiments, indicating that the FL-induced growth inhibition seen in *MLL*-rearranged cell lines results from induction of G_0-G_1 arrest, but not from apoptosis.

Phosphorylation of FLT3, STAT5, MAPK, and Akt is transiently up-regulated after FL stimulation in *MLL*-rearranged leukemia cells. It is known that FLT3 is dimerized after FL stimulation, and this evokes biological effects through the signaling pathways acting via STAT5, RAS/p44/42 MAPK, and phosphatidylinositol 3-kinase/Akt (26–28). To investigate activation patterns of signaling pathways after FL stimulation in *MLL*-rearranged cell lines, changes in phosphorylation of STAT5, MAPK, and Akt in KOCL-58 cells were pursued by Western blot using antibodies against the phosphorylated (active) form of these molecules. FLT3 phosphorylation was examined using anti-phosphotyrosine antibody after FLT3 immunoprecipitation. FLT3, STAT5, MAPK, and Akt were constitutively phosphorylated before FL stimulation as we reported previously (20), and their phosphorylation was further up-regulated within 1 min after FL stimulation (100 ng/mL) and returned to the prestimulated level at 15 min (Supplementary Fig. S2). A similar pattern of changes in phosphorylation of these molecules after FL stimulation was observed in KOPN-70, which showed a stimulative response to FL in the [^{3}H]thymidine uptake assay (data not shown), suggesting that an opposite biological

effect of FL, that is, stimulation or suppression of cell growth, is not simply due to differences in an early event of signaling after the FL/FLT3 interaction.

FL stimulation markedly up-regulates p27 expression in *MLL*-rearranged leukemia cells. It is known that cell cycle progression is controlled primarily by activities of CDKs that are up-regulated or down-regulated by cyclins and CDK inhibitors (CDKI), including p16, p21, and p27, respectively. To examine the expression of these cell cycle-associated proteins after FL stimulation, KOCL-58 cells (5×10^5/mL) were cultured 48 h in the presence or absence of FL (20 ng/mL). As shown in Fig. 2*A* (*left*), expression levels of cyclins A, B, D3, and E, and CDK2, CDK4, and CDK6, were completely unchanged. Expression of p16 was not detected as reported previously (23). Although expression of p21 was modestly up-regulated by FL, this was not seen consistently in repeated experiments. Of interest, expression of p27 was consistently and markedly up-regulated in the presence of FL. This p27 up-regulation was observed in a dose-dependent manner in response to FL, and reached a maximum level at 100 ng/mL (Fig. 2*A*, *top right*). In other experiments, it was shown that p27 was maximally up-regulated at FL concentrations between 20 and 40 ng/mL. Moreover, the FL-induced p27 up-regulation 48 h after FL stimulation was also observed to varying degrees in other *MLL*-rearranged cell lines with wild-type FLT3, but not in KOCL-33 with a D835 mutation (Fig. 2*A*, *bottom right*). Importantly, the FL-induced up-regulation of p27 was more profoundly observed in KOCL-58 and KOCL-50, which showed a marked suppression of [^{3}H]thymidine uptake by FL than in KOCL-45 and KOPN-1, which showed a modest suppression of [^{3}H]thymidine uptake by FL. In KOPN-55bi, KOPN-70 without *MLL* rearrangement that showed stimulative responses to FL, the p27 expression was somewhat down-regulated after FL stimulation.

To determine the mechanism of the FL-induced p27 up-regulation, changes in p27 mRNA expression after FL stimulation were examined in KOCL-58 by RNase protection assay. The level of p27 mRNA was completely unchanged after FL stimulation (Supplementary Fig. S3), suggesting that p27 up-regulation might be mediated by a posttranscriptional mechanism. To determine p27 stability, KOCL-58 cells were cultured for 48 h in the presence or absence of FL (20 ng/mL), further cultured after the addition of cycloheximide (150 μg/mL), and harvested 3, 6, and 9 h later. As shown in Fig. 2*B*, the estimated half-life of p27 was elongated from 2.6 h in the absence of FL to 3.9 h in the presence of FL. These results suggest that up-regulation of p27 induced by FL is due to suppression of its protein degradation.

Phosphorylation of STAT5 is specifically abrogated after FL stimulation in *MLL*-rearranged leukemia cells. To determine the activation status of FLT3-mediating signaling pathways at the time point where p27 is up-regulated by FL stimulation, KOCL-58 cells were cultured in the presence or absence of FL (20 ng/mL) for 48 h, and phosphorylation of STAT5, MAPK, and Akt was examined. As shown in Fig. 2*C*, in contrast to marked phosphorylation of STAT5 seen after 48 h of culture without FL, the addition of FL to the culture completely abrogated its phosphorylation. In contrast, phosphorylation of MAPK was up-regulated in the presence of FL at this time point, whereas phosphorylation of Akt showed no difference in the two culture conditions. This STAT5 dephosphorylation was observed in KOCL-58 within 1 h after FL stimulation (Fig. 2*D*). These results suggest that, among FLT3-mediating signaling pathways, the STAT5 pathway is specifically suppressed after FL stimulation.

FL stimulation renders *MLL*-rearranged leukemic cells resistant to anti-leukemic agent–induced apoptosis. It is thought that sensitivity of leukemia cells to irradiation and chemotherapeutic agents is reduced in "dormant" cells whose cell cycle progression is kept in sustained suppression. To assess whether the FL-induced cell cycle arrest affects sensitivity to irradiation-induced apoptosis, *MLL*-rearranged KOCL-58 and KOCL-51 cells (both possessing wild-type p53) were precultured for 24 h in the presence or absence of FL (20 ng/mL) and then irradiated (4 Gy). Induction of apoptosis was examined after 48 h of culture in the presence or absence of FL using FITC-conjugated Annexin V and propidium iodide. As shown in Fig. 3*A* (*left*), the Annexin V–positive apoptotic population decreased by FL from 45.3% to 24.5% in KOCL-58 and from 43.0% to 26.0% in KOCL-51. The propidium iodide–positive late apoptotic population also decreased in the presence of FL in both cell lines, suggesting that irradiation-induced apoptosis is effectively suppressed by pretreatment with FL followed by subsequent stimulation with FL. Similarly, to assess whether the FL-induced cell cycle arrest affects sensitivity to chemotherapeutic agent–induced apoptosis, KOCL-58 cells were precultured in the presence or absence of FL (20 ng/mL) for 24 h, and then exposed to daunorubicin (10 ng/mL) or AraC (200 nmol/L) for 48 h in the presence or absence of FL. As shown in Fig. 3*A* (*right*), the Annexin V–positive population decreased by FL from 38.1% to 20.5% in daunorubicin-treated cells and from 64.3% to 47.3% in AraC-treated cells. These results suggest that ligand activation of FLT3 in *MLL*-rearranged leukemia cells renders them resistant to irradiation- and chemotherapeutic agent–induced apoptosis.

To further evaluate the antiapoptotic activity of FL against chemotherapeutic agents in *MLL*-rearranged leukemia cells, KOCL-58 cells (4×10^4/well) were precultured for 24 h in the presence or absence of FL (20 ng/mL) and then cultured for 3 days with or without the addition of daunorubicin (10 ng/mL) or AraC (200 nmol/L). Numbers of living and dead cells were determined by the dye-exclusion method at days 2, 3, and 4 after the start of preculture (Fig. 3*B*). In the culture without the addition of daunorubicin or AraC (*top*), cell proliferation was gradually inhibited (~50% inhibition at day 4) in the presence of FL. Of note, in the culture to which either daunorubicin (*middle*) or AraC (*bottom*) was added, an increase in the dead cell population was markedly suppressed in the presence of FL (~50% suppression at days 3 and 4). The FL-mediating suppression of cell death was similarly observed at a higher concentration of daunorubicin or AraC (Fig. 3*C*). Thus, it was largely estimated that IC_{50} of daunorubicin and AraC was shifted by FL from 10 to 20 ng/mL and from 200 to 400 nmol/L, respectively. Of importance, the FL-induced inhibition of proliferation and resistance to AraC were specifically canceled by the addition of neutralizing anti-FL antibody in the culture medium (Fig. 3*D*, *left*). This FL effect was not observed in KOCL-33 with a D835 mutation (data not shown). These results indicate that the chemotherapeutic agent–induced apoptosis is suppressed *in vitro* via the interaction of FL with wild-type FLT3 in *MLL*-rearranged leukemia cells.

Coculture with bone marrow stromal cells renders *MLL*-rearranged leukemia cells chemoresistant, which is canceled by anti-FL antibody. Because FL is reported to be expressed at high levels as a soluble or membrane-bound form by bone marrow stromal cells (29), *MLL*-rearranged leukemia cells adhering to bone marrow stromal cells might be induced to cell cycle arrest via the FL/FLT3 interaction, resulting in acquisition of resistance to

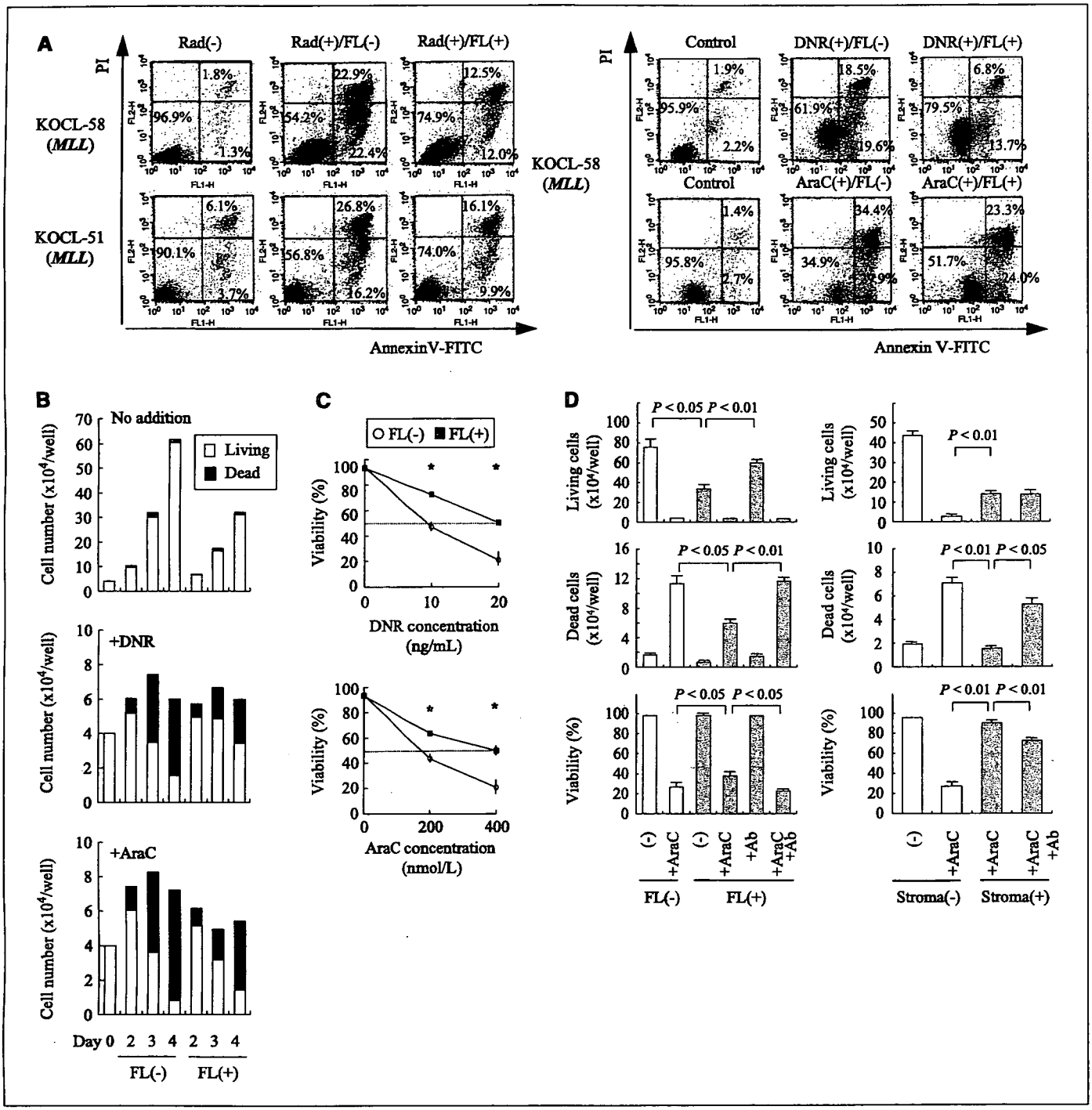

Figure 3. FL-induced resistance to antileukemic agents in *MLL*-rearranged leukemia cells. *A*, flow cytometric analysis of the FL effect on irradiation- and chemotherapeutic agent–induced apoptosis. KOCL-58 and KOCL51 cells were precultured for 24 h in the presence or absence of FL (20 ng/mL), and then irradiated (4 Gy) or exposed to daunorubicin (10 ng/mL) or AraC (200 nmol/L). Flow cytometric analysis was done 48 h later using FITC-conjugated Annexin V and propidium iodide. *Vertical* and *horizontal axes*, log fluorescence intensities of propidium iodide and FITC, respectively. Data are representative of three separate experiments. *B*, analysis of FL-induced resistance to chemotherapeutic agents in *MLL*-rearranged leukemia cells by dye-exclusion test. KOCL-58 cells (4×10^4/well) were precultured in the presence or absence of FL (20 ng/mL) for 24 h, and then cultured with or without daunorubicin (10 ng/mL) or AraC (200 nmol/L) for 3 d. *Columns*, mean numbers of living (*open columns*) and dead (*filled columns*) cells at days 2, 3, and 4 after the start of preculture. Data are representative of three separate experiments. *C*, FL-induced resistance to different concentrations of chemotherapeutic agents. KOCL-58 cells (4×10^4/well) were precultured in the presence or absence of FL (20 ng/mL) for 24 h, and then cultured with or without different concentrations of daunorubicin (10 and 20 ng/mL) or AraC (200 and 400 nmol/L) for 48 h. Viability was calculated by dye-exclusion test. *Points*, mean; *bars*, SE. *, $P < 0.05$, significant difference by *t* test. *D*, effect of anti-FL antibody on soluble FL or bone marrow stromal cell–induced resistance to chemotherapeutic agents. *Left*, KOCL-58 cells (4×10^4/well) were precultured in the presence (*filled columns*) or absence (*open columns*) of FL (20 ng/mL) for 48 h with or without the addition of anti-FL antibody (2 μg/mL), and then cultured with or without AraC (200 nmol/L) for 48 h. *Right*, KOCL-58 cells (4×10^4/well) were precultured with (*filled columns*) or without (*open columns*) KM-104 cells for 48 h in the presence or absence of anti-FL antibody (2 μg/mL), and then cultured with or without AraC (200 nmol/L) for 48 h. Living and dead cell numbers were counted in triplicate by dye-exclusion tests. *Columns*, representative mean from three separate experiments; *bars*, SE.

antileukemic agents. Using the bone marrow stromal cell line KM-104 expressing FL at high levels as the membrane form (Supplementary Fig. S4), we thus did the *in vitro* model study. KOCL-58 cells (4×10^4/well) were precultured for 2 days with or without KM-104 cells growing confluent on the bottom of the plate in the presence or absence of neutralizing anti-FL antibody (4 μg/mL), and then cultured in the presence or absence of AraC (200 nmol/L) for 2 days. As shown in Fig. 3*D* (*right*), the AraC-induced cell death was markedly ($P < 0.01$) suppressed when cocultured with stromal cells. Of importance, this stromal cell effect was partially but significantly canceled by anti-FL antibody in the culture medium, indicating that the FL/FLT3 interaction between *MLL*-rearranged leukemia cells and bone marrow stromal cells contributes, at least in part, to induction of cell cycle arrest of leukemia cells showing resistance to chemotherapeutic agents.

FL stimulation renders primary *MLL*-rearranged leukemic cells resistant to chemotherapeutic agent–induced cell death. To examine whether FL effect is also observed in primary *MLL*-rearranged leukemia cells, peripheral or bone marrow mononuclear cells (blasts >90%) stored in liquid nitrogen were thawed and used for experiments. Characteristics of primary leukemia samples with ($n = 9$) or without ($n = 5$) *MLL* rearrangement are summarized in Table 2. *MLL*-rearranged primary leukemia cells expressed FLT3 at significantly ($P < 0.01$) higher levels than did those without *MLL* rearrangement (median of positive population; 76% versus 25%; median of mean fluorescence intensity; 64.5 versus 30.4). Primary leukemia cells (1×10^5/well) were precultured for 24 h in the presence or absence of FL (40 ng/mL), further cultured for 24 h with AraC (100 nmol/L) in the presence or absence of anti-FL antibody (4 μg/mL), and harvested. As representatively depicted in Fig. 4*A* (case 1), the addition of FL rendered *MLL*-rearranged primary leukemia cells resistant to AraC, which was partially but significantly ($P < 0.05$) canceled by anti-FL antibody. The viabilities (%) after 48 h culture in 14 cases with or without *MLL* rearrangement are summarized in Table 2. Of note, the viabilities after AraC exposure significantly ($P < 0.05$) increased by the addition of FL in five of seven primary leukemia cells with *MLL* rearrangement, but not in five of five primary leukemia cells without *MLL* rearrangement. This FL effect was specifically canceled by anti-FL antibody in all of the cases tested. Statistically, the Δviabilities (treated viabilities − control viabilities) after AraC exposure significantly ($P < 0.05$) increased by the addition of FL, which was canceled by the addition of anti-FL antibody (Fig. 4*B*).

In six cases with *MLL* rearrangement, leukemia cells (1×10^5/well) were precultured for 24 h in the presence or absence of KM-104 cells with or without anti-FL antibody and further cultured for 24 h with AraC (100 nmol/L). As representatively depicted in Fig. 4*A* (case 8), coculture with bone marrow stromal cells rendered *MLL*-rearranged primary leukemia cells resistant to AraC, which was partially but significantly canceled by anti-FL antibody. The Δviabilities after AraC exposure significantly ($P < 0.05$) increased in the presence of stromal cells, which was canceled by the addition of anti-FL antibody (Fig. 4*C*). These results suggest that stimulation by FL, irrespective of its soluble or membrane form, specifically renders primary *MLL*-rearranged leukemia cells resistant to chemotherapeutic agent–induced cell death.

Discussion

MLL-rearranged infant ALL is known to have an especially poor prognosis (30), although its prognosis has gradually improved by intensified chemotherapy and hematopoietic stem cell transplantation (31–33). Nowadays, the complete remission rate in *MLL*-rearranged ALL after the induction chemotherapy has improved to

Table 2. Characteristics of B-precursor primary leukemia cells and their sensitivity to AraC and FLT3 expression

Case no.	Age (mo)/sex	WBC ($\times 10^3/\mu L$)	Sample		Karyotype/fusion gene	Viability (%) after 48 h culture*				FLT3 expression	
			Onset/relapse	BM/PB		Control	AraC	AraC + FL	AraC + FL + Ab	%	MFI
MLL rearrangement											
1	4/M	271	Onset	PB	t(4;11)	65 ± 4	46 ± 4	64 ± 2†	53 ± 2‡	91	64.5
2	1/M	42	Onset	PB	t(11;19)	57 ± 1	38 ± 1	50 ± 1†	40 ± 2‡	91	139.3
3	0/M	182	Relapse	BM	t(4;11)	61 ± 2	53 ± 2	59 ± 3	51 ± 3	70	76.5
4	5/M	440	Onset	PB	t(4;11)	55 ± 5	32 ± 3	45 ± 1†	34 ± 2‡	93	38.5
5	6/M	1,059	Onset	PB	t(4;11)	61 ± 1	54 ± 2	64 ± 2†	53 ± 3‡	92	74.8
6	3/F	40	Onset	PB	t(11;19)	57 ± 3	54 ± 1	58 ± 5	56 ± 2	43	43.3
7	0/M	350	Onset	PB	t(4;11)	51 ± 2	41 ± 2	56 ± 2†	47 ± 2‡	68	94.9
8	2/M	327	Relapse	PB	t(9;11)	66 ± 2	46 ± 3	NT	NT	70	33.4
9	5/F	225	Onset	PB	t(4;11)	63 ± 1	39 ± 4	NT	NT	76	41.3
MLL germ line											
10	56/M	88	Onset	PB	t(1;19)/*E2A-PBX1*	40 ± 2	26 ± 6	36 ± 6	33 ± 4	13	39.2
11	14/M	90	Onset	BM	t(1;19)/*E2A-PBX1*	46 ± 1	33 ± 4	33 ± 4	NT	40	20.3
12	28/M	59	Onset	PB	46,XX/*TEL-AML1*	66 ± 3	58 ± 6	53 ± 3	51 ± 3	7	19.4
13	34/F	9	Onset	PB	Hyperdiploid	66 ± 5	43 ± 1	51 ± 4	52 ± 6	39	32.2
14	18/F	51	Onset	PB	Hyperdiploid	55 ± 5	49 ± 2	47 ± 3	NT	25	30.4

Abbreviations: F, female; M, male; PB, peripheral blood; BM, bone marrow; Ab, neutralizing anti-FL antibody; NT, not tested.
*Data are shown as mean ± SE of triplicate wells.
† Significant increase ($P < 0.05$, t test) compared with AraC+.
‡ Significant decrease ($P < 0.05$, t test) compared with AraC+FL+.